The Journal of ExtraCorporeal Technology

Estimation of Hemoglobin Concentration at the Initiation of Cardiopulmonary Bypass Using Support Vector Regression

--Manuscript Draft--

Manuscript Number:	ject250087R1
Full Title:	Estimation of Hemoglobin Concentration at the Initiation of Cardiopulmonary Bypass Using Support Vector Regression
Article Type:	Original Article
Keywords:	hemoglobin; support vector regression; Cardiopulmonary Bypass; machine learning; hemodilution
Corresponding Author:	Makoto Hibiya, Ph.D. Fujita Health University: Fujita Ika Daigaku Toyoake, Aichi JAPAN
Corresponding Author Secondary Information:	
Corresponding Author's Institution:	Fujita Health University: Fujita Ika Daigaku
Corresponding Author's Secondary Institution:	
First Author:	Harutoyo Hirano, PhD
First Author Secondary Information:	
Order of Authors:	Harutoyo Hirano, PhD
	Shun Takahashi, Bachelor
	Tetsuya Kamei, PhD
	Makoto Hibiya, Ph.D.
Order of Authors Secondary Information:	
Abstract:	Background Hemodilution during cardiopulmonary bypass (CPB) is a standard perfusion strategy used to reduce blood viscosity and enhance microcirculatory flow. The hemodilution rate, expressed as hemoglobin (Hb) concentration, is a key control index in CPB and is currently estimated from total blood volume (TBV). The objective of this study was to propose a novel formula to accurately predict Hb concentration at the initiation of CPB (HbCPB), by incorporating circulating blood volume, laboratory data, physical measurements, and patient history. Methods We retrospectively analyzed 577 adult patients who underwent elective CPB at Fujita Health University Hospital from January 2016 to December 2020. Thirty-six preoperative variables—including demographics, laboratory data, circuit parameters, and indices such as TBV and ideal weight—were standardized. Categorical variables underwent one-hot encoding. We compared generalized linear models (GLM), support vector regression (SVR), and multilayer perceptron (MLP). Model performance was evaluated using the coefficient of determination (R2), mean squared error (MSE), and Bland–Altman analysis (bias and 95% limits of agreement, LoA). Predictions from two conventional TBV-based formulas were used as benchmarks. Results Of 993 screened cases, 577 met inclusion criteria (447 males, mean age 66.8 ± 11.7 years; 130 females, 69.5 ± 10.6 years). SVR on standardized predictors achieved the highest accuracy (R2 = 0.498, MSE = 0.517), outperforming GLM (R2 = 0.429,

	MSE=0.797) and MLP (R2 = 0.332, MSE=0.669). Conventional formulas showed lower performance (R2 = 0.325, MSE ≥ 1.48). Bland–Altman analysis for SVR demonstrated minimal bias (–0.0028g/dL) and narrower LoA (–1.42 to 1.41 g/dL) than conventional methods (bias –1.33 g/dL; LoA –3.49 to 0.83 g/dL). Conclusion These findings suggest that an SVR-based model improves prediction of HbCPB over conventional approaches, supporting optimized transfusion management and reduced hemodilution-related risks.
Response to Reviewers:	Response to comments of reviewers on the paper “Estimation of Hemoglobin Concentration at the Initiation of Cardiopulmonary Bypass Using Support Vector Regression” reference ject250087 First of all, the authors thank the reviewers for their comments. The reviewer’s concerns are addressed the attached file.

FUJITA HEALTH UNIVERSITY

Clinical and Educational Collaboration Unit, School of Medical Sciences, Fujita Health University
1-98, Dengakugakubo, Kutsukake-cho, Toyoake, Aichi, Japan, 470-1192
e-mail: mhibiya@fujita-hu.ac.jp
Tel: +81-562-93-2654

December 1st, 2025

Dr. Raymond K. Wong
Editor-in-Chief
The Journal of ExtraCorporeal Technology

Dear Dr. Raymond K. Wong

We wish to resubmit the attached manuscript (ject250087) entitled *"Estimation of Hemoglobin Concentration at the Initiation of Cardiopulmonary Bypass Using Support Vector Regression"* for consideration as an original article in the *Journal of ExtraCorporeal Technology*.

The resubmission includes our responses to the reviewers' comments (**Response_to_Reviewer.pdf**) and the revised manuscript with tracked changes (**Track_changes.pdf**), where modifications are highlighted in red. We sincerely thank you and the reviewers for your thoughtful suggestions and insights, which have enriched the manuscript and strengthened the presentation of our research.

Yours sincerely,

Makoto HIBIYA, Ph.D
Clinical and Educational Collaboration Unit, School of Medical Sciences, Fujita Health University
1-98, Dengakugakubo, Kutsukake-cho, Toyoake, Aichi, Japan, 470-1192
E-mail: mhibiya@shizuoka.ac.jp
Tel: +81-562-93-2654

[Reviewer 1]

Response to comments of **reviewer 1** on the paper "Estimation of Hemoglobin Concentration at the Initiation of Cardiopulmonary Bypass Using Support Vector Regression" reference ject250087

First of all, the authors thank the reviewer for their comments. The reviewer's concerns are addressed below.

●Comment (1)

This research article discusses the development of a new method for estimating hemoglobin concentration at the initiation of cardiopulmonary bypass (HbCPB). HbCPB is generally determined by total blood volume (calculated using height, weight, and/or BSA depending on the formula), priming volume and pre-CPB hemoglobin. The authors included other patient-related data such as laboratory data and clinical history along with the traditional component and employed three different training models to determine which model potentially performs better than other models and conventional methods. The authors found that their models perform slightly better than the conventional methods in predicting HbCPB. This manuscript provides a new concept of predicting HbCPB, which can perform better than the conventional formula and implies that other patient related components likely contribute to HbCPB. This manuscript is potentially publishable in JECT but requires major rewriting for JECT readers to appreciate their work better.

●Answer (1)

We are grateful for the reviewer's comprehensive assessment. Guided by these comments, we have revised the manuscript throughout and provided a point-by-point response below.

●Comment (2)

It seems to be beyond the capacity of JECT readers to understand the training models as described in the Materials and Methods section. The authors need to explain their "Analysis protocol" with plain language instead of scientific jargon. Most equations may not mean anything to JECT readers. The authors can remove several equations that are not necessary to explain their methodology in plain language.

Response (2)

In accordance with the reviewer's suggestion, we have substantially simplified the "Analysis Protocol," replacing technical jargon with plain language and removing equations that are not essential for understanding the methodology. We believe these revisions improve accessibility for JECT readers.

Before modification 2-1

P. 8

Linear model for hemoglobin concentration prediction at initiation of CPB

Conventional methods for estimating Hb_{CPB} at initiation (13, 14, 15) are typically classified as linear models. Linear modeling is appropriate when the relationship between explanatory variables and the target variable is approximately linear, or when a small number of predictors is used with a sufficiently large sample size. However, to the best of our knowledge,

no evidence confirms that a linear model is suitable for the variables used to estimate $\mathrm{Hb_{CPB}}$. The first hypothesis of this study was that a linear model would provide an adequate framework for estimating $\mathrm{Hb_{CPB}}$. A generalized linear model (GLM), a representative linear approach, is expressed by the following equation using explanatory variables $\mathbf{x}$ and a coefficient vector $\boldsymbol{\beta}$:

$$y = \beta_0 + \boldsymbol{\beta}^T\mathbf{x}, \quad \mathbf{x} = (x_1, x_2, \dots, x_P)^T, \quad \boldsymbol{\beta} = (\beta_1, \beta_2, \dots, \beta_P)^T \qquad (5)$$

GLM assumes a linear relationship between the explanatory variables and the target variable. However, when real-world data exhibit nonlinearities or complex interactions, predictive performance may deteriorate. This occurs because linear models cannot adequately capture such relationships, leading to large model errors.

The GLM defined in Equation (5) was fitted to $\mathrm{Hb_{CPB}}$ using either the standardized predictor matrix $\mathbf{X} \in \mathbb{R}^{N\times P}$ or the PCA-transformed score matrix $\mathbf{P} \in \mathbb{R}^{N\times P_{\mathrm{PCA}}}$. Parameter estimation was conducted by maximum likelihood under a Gaussian distribution with an identity link function, using MATLAB's fitglm function (MathWorks, Inc., Natick, MA, USA).

Nonlinear model for hemoglobin concentration prediction at initiation of CPB

The second hypothesis of this study was that nonlinear models would be more suitable for estimating $\mathrm{Hb_{CPB}}$. Therefore, two basic nonlinear models—support vector regression (SVR) and multilayer perceptron (MLP)—were evaluated. SVR constructs a regression function using a radial basis function (RBF) kernel. Given an input data matrix $X \in \mathbb{R}^{n\times d}$ and a target vector $y \in \mathbb{R}^n$, the RBF kernel is defined as

$$K(x_i, x_j) = \exp\left(-\frac{\| x_i - x_j\|^2}{2\sigma^2}\right). \quad (6)$$

A ε-SVR model is obtained by solving the convex optimization problem as follows:

$$\min_{w,b,\xi,\xi^*} \frac{1}{2}\|w\|^2 + C\sum_{i=1}^{n} \xi_i + \xi_i^*, \qquad (7)$$

$$\text{subject to } \begin{cases} y_i - (w^T\phi(x_i) + b) \le \varepsilon + \xi_i, \\ (w^T\phi(x_i) + b) - y_i \le \varepsilon + \xi_i^*, \\ \xi_i, \xi_i^* \ge 0, \quad i = 1, \dots, n, \end{cases}$$

where ϕ is the mapping to the feature space, C is the penalty constant (BoxConstraint), and ε is the width of the epsilon-insensitive zone. The predicted Hb concentration $\hat{y}(x)$ is then expressed as a linear combination of support vectors, as follows:

$$\hat{y}(x) = \sum_{i\in \boldsymbol{S}} \alpha_i, K(x_i, x) + b\,, \qquad \boldsymbol{S} = \{i|\alpha_i \ne 0\}. \qquad (8)$$

SVR can implicitly model complex nonlinear relationships in the input space through linear separation in a high-dimensional feature space. Its margin-maximization principle contributes to robust generalization performance. The multilayer perceptron (MLP) is a feedforward neural network with L - 1 hidden layers that employs nonlinear activation functions to approximate complex mappings (22). Given an input vector $\mathbf{X} \in \mathbb{R}^P$, the output of the lth layer is

$$\mathbf{h}^{(l)} = \phi\left(\mathbf{W}^{(l)}\mathbf{h}^{(l-1)} + \mathbf{b}^{(l)}\right), \ \mathbf{h}^{(0)} = \mathbf{X}. \qquad (9)$$

where $\mathbf{W}^l \in \mathbb{R}^{n_l\times n_{l-1}}$ and $\mathbf{b}^l \in \mathbb{R}^{n_l}$ are the weight and bias vectors of layer l, and $\phi(\cdot)$ is the activation function. The output layer performs a linear transformation of the last hidden layer output $\mathbf{h}^{(L-1)}$. The output $\hat{y} \in \mathbb{R}^k$ corresponding

to the Hb concentration at the initiation of CPB is expressed as follows:

$$\hat{\boldsymbol{y}} = \mathbf{W}^{(L)}\mathbf{h}^{(L-1)} + \mathbf{b}^{(L)}, \qquad (9)$$

where the parameters $\boldsymbol{W}^{(l)}, \boldsymbol{b}^{l}$ are learned via backpropagation or gradient descent methods. According to the universal approximation theorem, an MLP with a sufficiently large number of hidden units can approximate any continuous function, making it well-suited to capture complex nonlinearities and interactions. SVR was implemented to predict $\mathrm{Hb}_{\mathrm{CPB}}$ using either the standardized predictor matrix $\mathbf{X} \in \mathbb{R}^{N\times P}$ or the PCA-transformed score matrix $\mathbf{P} \in \mathbb{R}^{N\times P_{\mathrm{PCA}}}$. Model training was performed using MATLAB's fitrsvm function with the RBF kernel defined in Equation (6). The parameters (BoxConstraint C, kernel scale parameter σ, and epsilon-insensitive zone width ε in Equation (7) were optimized via 10-fold cross-validation using the expected-improvement-plus criterion. Model performance was evaluated using the cross-validated mean squared error (MSE) and the coefficient of determination (R^2).

The MLP was trained to predict $\mathrm{Hb}_{\mathrm{CPB}}$ using either the standardized predictor matrix $\mathbf{X} \in \mathbb{R}^{N\times P}$ or the PCA-transformed score matrix $\mathbf{P} \in \mathbb{R}^{N\times P_{\mathrm{PCA}}}$. A nested cross-validation scheme was employed: the data were divided into five outer folds ($K_{\mathrm{outer}} = 5$), and within each outer fold, a five-fold inner cross-validation ($K_{\mathrm{inner}} = 5$) was used to tune hyperparameters via grid search. The grid included hidden layer configurations: [4], [8], [16], [32], [32,16], [64,32], and [128,64]; training algorithms: Levenberg–Marquardt (23) and Resilient Backpropagation (24); learning rates: 10^{-3} and 10^{-4}; and early stopping tolerances: 10 and 20. The average MSE across the inner folds was used to select the optimal configuration. The final network was then retrained using the Levenberg–Marquardt algorithm with μ-control parameters (initial $\mu = 10^{-3}$, increase factor $\mu_{\mathrm{inc}} = 10$, decrease factor $\mu_{\mathrm{dec}} = 0.1$, maximum $\mu_{\mathrm{max}} = 10^{10}$), and L2 regularization with weight decay strength of 0.1 (25). To mitigate convergence to local minima, five random initializations were performed, and the model yielding the lowest validation MSE was retained. Model performance was reported as the outer-fold MSE and coefficient of determination (R^2).

After modification 2-1

P. 8

Linear model for predicting hemoglobin concentration at CPB initiation

Conventional methods for estimating $\mathrm{Hb}_{\mathrm{CPB}}$ (17–19) are essentially linear models that incorporate a limited set of patient and circuit factors, such as priming volume. We first evaluated whether a linear approach would be adequate for our dataset. To do so, we fit a generalized linear model (GLM) using routinely available pre-CPB variables, including body size indices, laboratory values, and circuit settings. The GLM assumes that $\mathrm{Hb}_{\mathrm{CPB}}$ varies in approximate proportion to changes in these inputs. Model performance was assessed using the coefficient of determination (R^2) and mean squared error (MSE). The explicit GLM equation and estimation procedures are provided in Supplementary Equation (S-i).

Nonlinear model for predicting hemoglobin concentration at CPB initiation

Because clinical data often contain nonlinear relationships and interactions that linear models may not capture, we also evaluated two standard nonlinear approaches: Support Vector Regression (SVR) and a Multilayer Perceptron (MLP).

SVR can model curved relationships between the inputs and $\mathrm{Hb}_{\mathrm{CPB}}$ without the need to specify functional forms. We used a widely adopted SVR implementation and tuned its hyperparameters by cross-validation to reduce overfitting;

further details are provided in the Supplement (equations s-ii, iii). The MLP is a simple neural-network model that learns patterns by stacking a small number of layers. We compared several compact architectures and training configurations and selected the model that performed best in cross-validation. Training details (architecture and stopping criteria) are summarized in the Supplement (equation s-iv).

For some analyses, we also used a compressed set of input variables derived from principal component analysis to reduce redundancy among predictors. We retained the smallest number of components that preserved approximately 90% of the total variance. Technical details are provided in Supplement S2.

Model training, validation, and reporting

For all models, we standardized inputs when appropriate, tuned model settings by cross-validation, and summarized performance using R^2 and MSE. Because correlation-based indices do not measure exact agreement, we also evaluated agreement between predicted and measured $\mathrm{Hb}_{\mathrm{CPB}}$ with Bland–Altman analysis (bias and 95% limits of agreement).

Software and reproducibility

Analyses were performed with commonly used, **off-the-shelf software** (e.g., MATLAB equivalents or open-source alternatives). Parameter settings and code snippets sufficient for reproduction are listed in the Supplement.

Addition 2-2

P. 26

Supplemental Material

S1. Generalized Linear Model (GLM)

For standardized predictors $X \in \mathbb{R}^{N\times P}$ and target $y \in \mathbb{R}^{N}(\mathrm{Hb}_{\mathrm{CPB}})$, we fit a Gaussian-identity GLM:

$$y = \beta_0 + X\beta + \varepsilon, \qquad \varepsilon \sim \mathcal{N}(0, \sigma^2 I) \qquad (\mathrm{s}-\mathrm{i})$$

Parameters (β_0, β) were estimated by maximum likelihood (equivalently, least squares under (i)). Implementation used MATLAB fitglm (MathWorks) with default options.

S2. Support Vector Regression (SVR)

We used ε-SVR with radial basis function (RBF) kernel as shown in the following equation:

$$K(x_i, x_j) = \exp\left(-\frac{\| x_i - x_j \|^2}{2\sigma^2}\right). \qquad (\mathrm{s}-\mathrm{ii})$$

A ε-SVR model is obtained by solving the convex optimization problem as follows:

$$\min_{w,b,\xi,\xi^*} \frac{1}{2}\|w\|^2 + C\sum_{i=1}^{n} \xi_i + \xi_i^*, \qquad (\mathrm{s}-\mathrm{iii})$$

$$\text{subject to} \begin{cases} y_i - (w^T\phi(x_i) + b) \le \varepsilon + \xi_i, \\ (w^T\phi(x_i) + b) - y_i \le \varepsilon + \xi_i^*, \\ \xi_i, \xi_i^* \ge 0, \quad i = 1, \dots, n, \end{cases}$$

where ϕ is the mapping to the feature space, C is the penalty constant (BoxConstraint), and ε is the width of the epsilon-

insensitive zone. The predicted Hb concentration $\hat{y}(x)$ is then expressed as a linear combination of support vectors, as follows:

$$\hat{y}(x) = \sum_{i \in \boldsymbol{S}} \alpha_i, K(x_i, x) + b\,, \qquad \boldsymbol{S} = \{i | \alpha_i \neq 0\}. \qquad (\mathrm{s-iv})$$

We tuned $(C, \sigma, \gamma, \varepsilon)$ by cross-validation. Implementation used MATLAB fitrsvm with RBF kernel; expected-improvement-plus criterion in 10-fold CV guided selection.

S3. Multilayer Perceptron (MLP)

We used a feed-forward network with $L-1$ hidden layers. For an input $x \in \mathbb{R}^P$, the layer outputs were defined as:

$$\mathbf{h}^{(l)} = \phi\left(\mathbf{W}^{(l)}\mathbf{h}^{(l-1)} + \mathbf{b}^{(l)}\right), \qquad \mathbf{h}^{(0)} = \mathbf{X}. \qquad (\mathrm{s-v})$$

with the final prediction given by:

$$\hat{\boldsymbol{y}} = \mathbf{W}^{(L)}\mathbf{h}^{(L-1)} + \mathbf{b}^{(L)}, \qquad (\mathrm{s-vi})$$

The weights $\{W^{(\ell)}, b^{(\ell)}\}$ were learned by backpropagation using either the Levenberg–Marquardt or Resilient Backpropagation algorithm (31, 32), with learning rates 10^{-3}or $10^{-4}$and early-stopping patience of 10 or 20 epochs. Model selection followed a nested cross-validation scheme with 5 outer folds and a 5-fold inner grid search over hidden-layer sizes $[4], [8], [16], [32], [32,16], [64,32], [128,64]$, algorithm $\in$ {LM,RProp}, learning rate $\in \{10^{-3}, 10^{-4}\}$, and early-stopping tolerance $\in \{10,20\}$. On the full standardized predictor matrix X, the selected configuration was $[4]$(one hidden layer with 4 neurons) trained with LM at a learning rate of 10^{-3}, early stopping of 10 epochs, and L2 weight decay of 0.1 (33); five random initializations were run and the model with the lowest validation MSE was retained.

S4. Dimensionality Reduction via PCA.

Continuous variables were z-score standardized and categorical variables were one-hot encoded. Principal component analysis (PCA) was then applied to the full predictor matrix to obtain the score matrix $P \in \mathbb{R}^{N \times P_{\mathrm{PCA}}}$. The retention rule was prespecified as "keep the smallest number of components whose cumulative explained variance reaches at least 90%." Component loadings were computed to support interpretability.

S5. Cross-validation, Metrics, and Comparative Baselines.

For model validation, SVR/MPL used standard train–validation splits with reporting on the final fit; SVR employed 10-fold cross-validation for hyperparameter selection and cross-validated error estimates; and MLP used nested 5×5 cross-validation for model selection with outer-fold performance reported. Model performance was summarized uniformly using R^2 and MSE, and agreement between predicted and measured values was assessed with Bland–Altman analysis (bias and 95% limits of agreement). Two published TBV-based formulas were included as comparative baselines; all models (baselines and proposed) were evaluated under the same preprocessing and validation procedures.

•Comment (3)

Additionally, equation numbering is confusing with the reference numbering. Equation numbering should be different from the reference numbering (a, b, c and so on or I, ii, iii …).

Response (3)

In accordance with the reviewer's suggestion, we have reformatted all equation numbering to i, ii, iii, … throughout the manuscript to avoid any confusion with the reference numbering.

Before modification 3-1

P. 6

BMI, ideal body weight (BW_i)(14), TBV (11) and BSA (17) were calculated as follows (Equations (1)–(4)):

$$BMI = \frac{w}{h^2}, \quad (1)$$

$$BW_i = 22h^2, \quad (2)$$

$$TBV = 80w, \quad (3)$$

$$BSA = 0.7184 \times 10^{-4} \times h^{0.725} \times w^{0.425}, \quad (4)$$

After modification 3-1

P. 6

BMI, ideal body weight (BW_i)(14), TBV (11) and BSA (17) were calculated as follows (Equations (i)–(iv)):

$$BMI = \frac{w}{h^2}, \quad (i)$$

$$BW_i = 22h^2, \quad (ii)$$

$$TBV = 80w, \quad (iii)$$

$$BSA = 0.7184 \times 10^{-4} \times h^{0.725} \times w^{0.425}, \quad (iv)$$

Before modification 3-2

P. 12

To benchmark our method against conventional prediction models, the same clinical dataset was fitted using the standard hematocrit-based prediction formula (14), which is expressed as:

$$\mathrm{Ht_{CPB}} = \mathrm{Ht_{beforeCPB}} \times \left(1 - \frac{\mathrm{PV}}{\mathrm{PV+TBV}}\right), \quad (11)$$

where $\mathrm{Ht_{CPB}}$ is the hematocrit value under CPB, $\mathrm{Ht_{beforeCPB}}$ is the hematocrit value before CPB, PV is Priming Volume. TBV was substituted from two approaches: Equation (3) (15) and the following equation (14):

$$\mathrm{TBV} = \begin{cases} 70 \times \mathrm{BW} & (\mathrm{Age} < 65) \\ 60 \times BW & (\mathrm{Age} \geq 65) \end{cases}, \quad (12)$$

Estimated Hb concentrations based on Equation (11) and their Bland–Altman statistics, mean difference, and 95 % LoA, were compared with those obtained for our approach.

After modification 3-2

P. 11

To benchmark our method against conventional prediction models, the same clinical dataset was fitted using the standard hematocrit-based prediction formula (14), which is expressed as:

$$\mathrm{Ht_{CPB}} = \mathrm{Ht_{beforeCPB}} \times \left(1 - \frac{\mathrm{PV}}{\mathrm{PV+TBV}}\right), \quad (v)$$

where Ht_{CPB} is the hematocrit value under CPB, $Ht_{beforeCPB}$ is the hematocrit value before CPB, PV is Priming Volume. TBV was substituted from two approaches: Equation (iii) (15) and the following equation (14):

$$TBV = \begin{cases} 70 \times BW & (Age < 65) \\ 60 \times BW & (Age \geq 65) \end{cases}, \quad \text{(vi)}$$

Estimated Hb concentrations based on Equation (v) and their Bland–Altman statistics, mean difference, and 95 % LoA, were compared with those obtained for our approach.

Before modification 3-3

P. 12

Conversely, biases from conventional models were confirmed (reference (11): $p < 0.01, d = -1.21$; Equation (11): $p < 0.01, d = -0.617$).

After modification 3-3

P. 14

Conversely, biases from conventional models were confirmed (reference (11): $p < 0.01, d = -1.21$; Equation (xi): $p < 0.01, d = -0.617$).

•Comment (4)

Even though authors employed complicated training models, PC1 contributes 20% and PC1 to PC4 contribute to 50% (I assume that dots in Figure 2 represent PC1 through PC17 from left to right, which needs to be described in the figure legend). Components of PC1 and PC2 are mainly weight, height, TBV, BSA, BMI, ideal weight, and obesity. It indicates that total blood volume based on weight, height and/or BSA is still the most important component in estimating HbCPB in their models. I am not sure whether the authors are able to identify other components that improved the HbCPB prediction in their models compared to the conventional formula.

Response (4)

We appreciate the reviewer's insightful observation. We have revised the Figure 2 legend to explicitly state that the dots represent the cumulative inclusion of PCs (PC1 to PC17 from left to right). We agree that PC1 and PC2 are predominantly composed of weight, height, TBV, BSA, BMI, ideal weight, and obesity, supporting the interpretation that TBV-related factors remain central to Hb_{CPB} estimation. Although our models incorporating PCs 1–17 outperformed the conventional formula, we cannot presently attribute this improvement to specific PCs without further ablation or feature-contribution analyses. We have added this clarification to the Limitations section and plan to address it in future work.

Before modification 4-1

P. 6

Figure 2: Cumulative contribution rate. Top 17 principal components were required to achieve 90 % cumulative explained variance.

After modification 4-1

P. 6

Figure 2. Cumulative explained variance. PCs are added sequentially from PC1 to PC17 (left to right); 90% cumulative explained variance is achieved with the first 17 PCs.

Before modification 4-2

P. 16

In this study, the first 17 principal components were adopted, collectively accounting for 90％ of the cumulative contribution rate in the predictor matrix. While this approach preserved most of the predictor information, it may have failed to isolate features most relevant to Hb_{CPB}. Furthermore, the first principal component accounted for more than 20％ of the total variance, indicating the presence of latent factors common to blood laboratory data and patient background characteristics that drive coherent variation across multiple variables. As a result, the PCR model may not have adequately captured the most predictive features of Hb_{CPB}, which likely contributed to its reduced performance, as reflected in the lower coefficient of determination and higher MSE compared with the GLM using the full predictor set. Traditional predictors used to estimate Hb_{CPB}—including body weight, priming volume (static circuit volume), and preoperative Hb concentration--- were embedded within the principal components retained by PCR and were selected as input features for both the SVR and MLP models. Nevertheless, several of the principal components used in Hb_{CPB} prediction did not primarily reflect these conventional parameters. Therefore, Hb_{CPB} cannot be fully explained by body weight, priming volume, and preoperative Hb concentration alone, as suggested by conventional approaches. These findings highlight the influence of additional confounding variables, including age and comorbidities.

After modification 4-2

P. 15

In this study, the first 17 principal components were adopted, collectively accounting for 90% cumulative explained variance in the predictor matrix. While this approach preserved most of the predictor information, it may have failed to isolate features most relevant to Hb_{CPB}. Furthermore, the first principal component accounted for more than 20% of the total variance, and PC1 and PC2 were primarily composed of weight, height, TBV, BSA, BMI, ideal weight, and obesity measures, supporting the interpretation that TBV-related factors remain central to Hb_{CPB} estimation. As a result, the PCR model may not have adequately captured the most predictive features of Hb_{CPB}, likely contributing to its reduced performance, as reflected in the lower coefficient of determination and higher MSE compared with the GLM using the full predictor set. Traditional predictors used to estimate Hb_{CPB}—including body weight, priming volume (static circuit volume), and preoperative Hb concentration—were embedded within the principal components retained by PCR and were selected as input features for both the SVR and MLP models. Nevertheless, several of the principal components used in Hb_{CPB} prediction did not primarily reflect these conventional parameters. Therefore, Hb_{CPB} cannot be fully explained by body weight, priming volume, and preoperative Hb concentration alone, as suggested by conventional approaches. At the same time, while models using PCs 1–17 showed better performance than the conventional formula, we cannot presently ascribe the improvement to specific components without dedicated ablation or feature-contribution analyses. These findings highlight the influence of additional confounding variables, including

age and comorbidities.

Addition 4-3

P. 18

Limitations

While the proposed models using PCs 1–17 outperformed the conventional formula, we cannot, at present, attribute this improvement to specific principal components without dedicated ablation or feature-contribution analyses. We acknowledge this as a limitation and plan to investigate the contribution of individual components and underlying variables in future work.

●Comment (5)

All scattered plots in Figure 4 need linear regression analysis to provide the slope and Y-intercept. Better estimation of HbCPB will result in the slope close to 1 and Y-intercept close to 0. R or R2 are indicating the correlation but not the exact match. Just by eyeballing, the slope is likely higher than 1 in Figure2 a, b, and c while lower than 1 in Figure 2 d and e. Authors used both R in Figure 4 and R2 in other places. It should be better to use only one to be consistent.

Response (5)

In accordance with the reviewer's recommendation, we have added ordinary least-squares linear regression analyses to all scatter plots in Figure 4 and have reported the slope and y-intercept for each panel. We agree that a slope close to 1 and an intercept close to 0 better reflect accurate estimation. Our results showed that the slopes in Figures 2(a), 2(b), and 2(c) were close to 1, whereas those in Figures 2(d) and 2(e) were not. Because R and R^2 quantify correlation and model fit rather than agreement, we further assessed accuracy using Bland–Altman bias and limits of agreement (Figure 5). To avoid confusion and ensure consistency, all correlation metrics throughout the manuscript are now reported exclusively as R^2.

Before modification 5-1

P. 14

Figure 4 shows the comparison between measured $\mathrm{Hb_{CPB}}$ and predicted values based on pre-CPB variables, while Table 3 summarizes model performance indices. A GLM fitted to the standardized predictor matrix $\mathbf{X} \in \mathbb{R}^{N\times P}$ achieved a coefficient of determination of $R^2_{\mathrm{GLM}} = 0.429$, adjusted $R^2_{\mathrm{GLM}} = 0.369$, and $\mathrm{MSE_{GLM}} = 0.797$. However, multicollinearity in the input matrix was confirmed, resulting in a lack of full rank. Applying the same GLM to PCA-transformed predictors $\mathbf{X}_{\mathrm{PCA}} \in \mathbb{R}^{N\times P_{\mathrm{PCA}}}$ yielded $R^2_{\mathrm{PCR}} = 0.371$ (adjusted $R^2_{\mathrm{PCR}} = 0.352$) and $\mathrm{MSE_{PCR}} = 0.808$. SVR on $\mathbf{X}$ with optimized hyperparameters $C = 2.279$, $\gamma = 16.81$, and $\varepsilon = 0.594$ yielded $R^2_{\mathrm{SVR}} = 0.498$ and 10-fold CV $\mathrm{MSE_{SVR}} = 0.517$, outperforming the GLM. When SVR was applied to $\mathbf{X}_{\mathrm{PCA}}$ with $C = 1.662$, $\gamma = 14.28$, and $\varepsilon = 0.0084$, performance decreased to $R^2_{\mathrm{SVR_{PCA}}} = 0.39$ and CV $\mathrm{MSE_{SVR_{PCA}}} = 0.52$. The MLP model, tuned via nested 5-fold CV, selected one hidden-layer architecture of 4 neurons, with Resilient Backpropagation, a learning rate of 10^{-3}, and early stopping tolerance of 10. On $\mathbf{X}$, this configuration yielded $R^2_{\mathrm{MLP}} = 0.332 \pm 0.033$ and $\mathrm{MSE_{MLP}} = 0.669 \pm 0.086$. When

applied to $\mathbf{X}_{\mathrm{PCA}}$, the MLP achieved R^2 = 0.352 ± 0.054 and MSE = 0.646 ± 0.068. The coefficients of determination from both MLP configurations were lower than those from SVR. Previously published $\mathrm{Hb}_{\mathrm{CPB}}$ prediction formulas yielded R^2 = 0.3225, MSE = 2.98 based on (15), and R^2 = 0.3245, MSE = 1.48 based on (14), both substantially lower than SVR performance.

After modification 5-1

P. 12

Figure 4 shows the comparison between measured $\mathrm{Hb}_{\mathrm{CPB}}$ and predicted values based on pre-CPB variables, while Table 3 summarizes model performance indices. For each scatter plot in Figure 4, the ordinary least-squares regression slopes and y-intercepts—where better estimation is reflected by a slope close to 1 and a y-intercept close to 0—are displayed. The slopes and intercepts (panels a–e) are as follows: (a) slope = 1.00, intercept = 4.00×10^{-5}; (b) slope = 1.22, intercept = −1.88; (c) slope = 0.92, intercept = 0.68; (d) slope = 0.44, intercept = 4.18; (e) slope = 0.48, intercept = 4.13. A GLM fitted to the standardized predictor matrix $X \in R^{N \times P}$ achieved a coefficient of determination of R^2_{GLM} = 0.429, adjusted R^2_{GLM} = 0.369, and $\mathrm{MSE}_{\mathrm{GLM}}$ = 0.797. However, multicollinearity in the input matrix was confirmed, resulting in a lack of full rank. Applying the same GLM to PCA-transformed predictors $X_{PCA} \in R^{N \times P_{PCA}}$ yielded R^2_{PCR} = 0.371 (adjusted R^2_{PCR} = 0.352) and $\mathrm{MSE}_{\mathrm{PCR}}$ = 0.808. SVR on X with optimized hyperparameters C = 2.279, γ = 16.81, and ε = 0.594 yielded R^2_{SVR} = 0.498 and 10-fold CV $\mathrm{MSE}_{\mathrm{SVR}}$ = 0.517, outperforming the GLM. When SVR was applied to X_{PCA} with C = 1.662, γ = 14.28, and ε = 0.0084, performance decreased to $R^2_{SVR_{PCA}}$ = 0.39 and CV $MSE_{SVR_{PCA}}$ = 0.52. The MLP model, tuned via nested 5-fold CV, selected one hidden-layer architecture of 4 neurons, with Resilient Backpropagation, a learning rate of 10^{-3}, and early stopping tolerance of 10. On X, this configuration yielded R^2_{MLP} = 0.332 ± 0.033 and $\mathrm{MSE}_{\mathrm{MLP}}$ = 0.669 ± 0.086. When applied to X_{PCA}, the MLP achieved R^2 = 0.352 ± 0.054 and MSE = 0.646 ± 0.068. The coefficients of determination from both MLP configurations were lower than those from SVR. Previously published Hb_{CPB} prediction formulas yielded R^2 = 0.3225, MSE = 2.98 based on (19), and R^2 = 0.3245, MSE = 1.48 based on (18), both substantially lower than SVR performance.

Before modification 5-2

P. 5

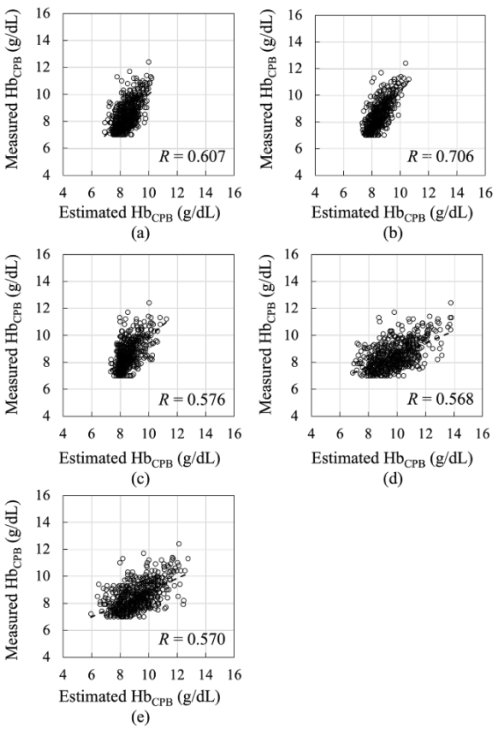

After modification 5-2

P. 5

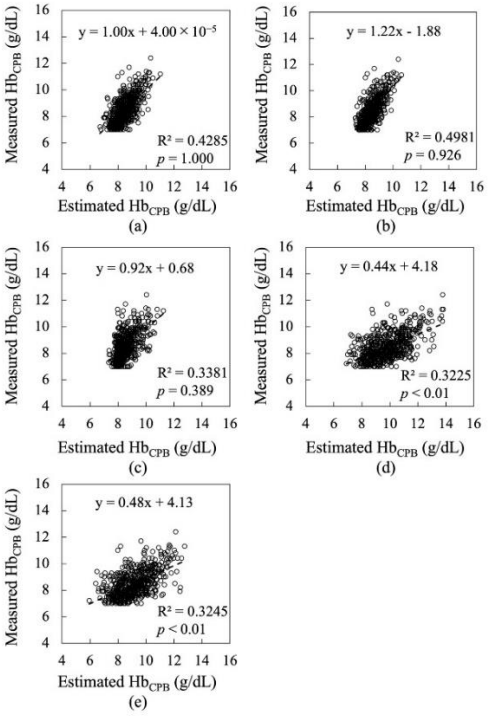

●Comment (6)

P2 in abstract "This objective of this study". The objective?

Response (6)

We acknowledge that this issue resulted from a typographical error. We apologize for the oversight and have corrected it in the revised manuscript. Kindly verify the updated version.

Before modification 6-1

P. 2

This objective of this study was to propose a novel formula to accurately predict Hb concentration at the initiation of CPB (Hb_{CPB}), by incorporating circulating blood volume, laboratory data, physical measurements, and patient history.

After modification 6-1

P. 2

The objective of this study was to propose a novel formula to accurately predict Hb concentration at the initiation of CPB (Hb_{CPB}), by incorporating circulating blood volume, laboratory data, physical measurements, and patient history.

●Comment (7)

P2 in abstract, "PCA" is not well defined and not used again in the abstract.

Response (7)

We appreciate the reviewer's observation. To avoid introducing an undefined acronym and to improve the clarity of the abstract, we have removed the reference to PCA and revised the wording accordingly.

Before modification 7-1

P. 2

We compared generalized linear models (GLM), support vector regression (SVR), and multilayer perceptron (MLP), each trained on the full predictor set and on principal components (PCA; cumulative variance ≥ 90%). Model performance was evaluated using the coefficient of determination (R^2), mean squared error (MSE), and Bland–Altman analysis (bias and 95% limits of agreement, LoA). Predictions from two conventional TBV-based formulas were used as benchmarks.

After modification 7-1

P. 2

We compared generalized linear models (GLM), support vector regression (SVR), and multilayer perceptron (MLP)~~, each trained on the full predictor set and on principal components (PCA; cumulative variance ≥ 90%)~~. Model performance was evaluated using the coefficient of determination (R^2), mean squared error (MSE), and Bland–Altman analysis (bias and 95% limits of agreement, LoA). Predictions from two conventional TBV-based formulas were used as benchmarks.

●Comment (8)

P4 in introduction "Hemodilution during CPB is a standard perfusion strategy used to reduce blood viscosity and enhance microcirculatory flow" needs references

Response (8)

In response to the reviewer's comment, we have added the relevant references and updated the manuscript accordingly. We would appreciate the reviewer's confirmation.

Before modification 8-1

P. 4

Hemodilution during CPB is a standard perfusion strategy used to reduce blood viscosity and enhance microcirculatory flow.

After modification 8-1

P. 4

Hemodilution during CPB is a standard perfusion strategy used to reduce blood viscosity and enhance microcirculatory flow (5).

Addition 8-2

P. 21

(5) Taniguchi FP, Martins AS. Hemodilution, kidney dysfunction and cardiac surgery. Einstein (Sao Paulo). 2009;7(1 Pt 1):103-7.

●Comment (9)

P4 in introduction "However, anemia resulting from hemodilution may cause ischemic organ injury, increase mortality, and elevate stroke risk" needs references

Response (9)

In response to the reviewer's comment, we have added the relevant references and updated the manuscript accordingly. We would appreciate the reviewer's confirmation.

Before modification 9-1

P. 4

However, anemia resulting from hemodilution may cause ischemic organ injury, increase mortality, and elevate stroke risk

After modification 9-1

P. 4

However, anemia resulting from hemodilution may cause ischemic organ injury, increase mortality, and elevate stroke risk (6, 7, 8).

Addition 9-2

P. 21

(6) Ranucci M, Conti D, Castelvecchio S, et al. Hematocrit on cardiopulmonary bypass and outcome after coronary surgery in nontransfused patients. Ann Thorac Surg. 2010; 89 (1): 11-17. (7) Karkouti K, Djaiani G, Borger MA, et al. Low hematocrit during cardiopulmonary bypass is associated with increased risk of perioperative stroke in cardiac surgery. Ann Thorac Surg. 2005; 80(4): 1381-1387. (8) Tsui AKY, Dattani ND, Marsden PA, et al. Reassessing the risk of hemodilutional anemia: Some new pieces to an old puzzle. Can J Anaesth. 2010; 57(8): 779-791.

●Comment (10)

P7 in Analysis protocol "One-hot encoding was applied to 15 categorical variables (e.g., sex, type of surgery, and presence of comorbidities), and z-score standardization was applied to 20 continuous variables (e.g., laboratory data)." neesd references

Response (10)

In response to the reviewer's comment, we have added the relevant references and updated the manuscript accordingly. We would appreciate the reviewer's confirmation.

Before modification 10-1

P. 7

One-hot encoding was applied to 15 categorical variables (e.g., sex, type of surgery, and presence of comorbidities), and z-score standardization was applied to 20 continuous variables (e.g., laboratory data).

After modification 10-1

P. 7

One-hot encoding was applied to 15 categorical variables (e.g., sex, type of surgery, and presence of comorbidities), and z-score standardization was applied to 20 continuous variables (e.g., laboratory data) (24, 25).

Addition 10-2

P. 24

(24) Maharana K, Mondal S, Nemade B. A review: Data pre-processing and data augmentation techniques. Global Transitions Proceedings. 2022; 3(1): 91-99.

(25) Hancock JT, Khoshgoftaar TM. Survey on categorical data for neural networks. J Big Data. 2020; 7: 28.

●Comment (11)

P15 in Bland-Altman analysis, bias and LoA of Figure 5 a, b, c, and d are described but not e.

Response (11)

We acknowledge the omission and apologize for the oversight. We have added the Bland–Altman bias and limits of agreement for Figure 5e and updated the corresponding description. Kindly verify the changes.

Before modification 11-1

P. 15

Figure 5 displays the Bland–Altman analysis results. The bias between predicted and measured GLM values was $–5\times10^{-7}$ g/dL (95% CI: -0.0654 to 0.0654 g/dL), with 95% LoA of [–1.57 g/dL, 1.57 g/dL]. For SVR, the bias was –0.0028g/dL (95% CI: -0.0619 to 0.0562g/dL) with LoA of [–1.41 g/dL, 1.41 g/dL]. For MLP, the bias was –0.029 g/dL (95% CI: -0.0963 to 0.0375g/dL), and LoA was [–1.63 g/dL, 1.57 g/dL]. In contrast, the conventional method had a bias of –1.33 g/dL (95% CI: –1.41 to –1.24 g/dL) and LoA of [–3.49 g/dL, 0.831 g/dL]. The 95% CI for bias did not include zero, indicating systematic error. In comparison, CIs from GLM, SVR, and MLP included zero, suggesting no statistically significant bias and the absence of systematic error. Biases between measured and predicted Hb_{CPB} from GLM, SVR, and MLP were not statistically significant (GLM: $p = 1.000$, $d = -6.5\times10^{-7}$; SVR: $p = 0.926$, $d = -0.004$; MLP: $p = 0.389$, $d = -0.036$). Conversely, biases from conventional models were confirmed (reference (11): $p < 0.01$, $d = -1.21$; Equation (11): $p < 0.01$, $d = -0.617$).

After modification 11-1

P. 14

Figure 5 displays the Bland–Altman analysis results. The bias between predicted and measured GLM values was $–5\times10^{-7}$ g/dL (95% CI: -0.0654 to 0.0654 g/dL), with 95% LoA of [–1.57 g/dL, 1.57 g/dL]. For SVR, the bias was –0.0028g/dL (95% CI: -0.0619 to 0.0562g/dL) with LoA of [–1.41 g/dL, 1.41 g/dL]. For MLP, the bias was –0.029 g/dL (95% CI: -0.0963 to 0.0375g/dL), and LoA was [–1.63 g/dL, 1.57 g/dL]. In contrast, the conventional methods had a bias of –1.33 g/dL (95% CI: –1.41 to –1.24 g/dL) and LoA of [–3.49 g/dL, 0.831 g/dL] for the reference (11) and a bias of –0.64 g/dL (95% CI: –0.72 to –0.555 g/dL) and LoA of [–2.67g/dL, 1.39g/dL] for the Equation (v), respectively. The 95% CI for bias did not include zero, indicating systematic error. In comparison, CIs from GLM, SVR, and MLP included zero, suggesting no statistically significant bias and the absence of systematic error. Biases between measured and predicted Hb_{CPB} from GLM, SVR, and MLP were not statistically significant (GLM: $p = 1.000$, $d = -6.5\times10^{-7}$; SVR: $p = 0.926$, $d = -0.004$; MLP: $p = 0.389$, $d = -0.036$). Conversely, biases from conventional models were confirmed (reference (11): $p < 0.01$, $d = -1.21$; Equation (v): $p < 0.01$, $d = -0.617$).

●Comment (12)

The Reference section is not organized in the JECT format.

Response (12)

In accordance with the reviewer's comment, we have reformatted the Reference section to comply with the JECT guidelines. In addition, former item (10), which cited a handbook, has been replaced with an original research article, and the in-text citations and numbering have been updated accordingly. We would appreciate the reviewer's confirmation.

Before modification 12-1

P. 20

(1) Hirata Y, Hirahara N, Murakami A, Motomura N, Miyata H, Takamoto S. Current status of cardiovascular surgery in Japan: analysis of data from Japan Cardiovascular Surgery Database in 2015, 2016.Japanese Journal of Cardiovascular Surgery. 2019; 48(1): 1-5.

(2) Tomonobu A, Kiyoharu N, Norimichi H, Noboru M, Hiroaki M, Shin'ichi T. Current Status of Cardiovascular Surgery in Japan: Analysis of Data from Japan Cardiovascular Surgery Database in 2015, 2016. Japanese Journal of Cardiovascular Surgery. 2019; 48(1): 11-7.

(3) Shimizu H, Hirahara N, Motomura N, Miyata H, Takamoto S. Current Status of Cardiovascular Surgery in Japan: Analysis of Data from Japan Cardiovascular Surgery Database in 2015, 2016. Japanese Journal of Cardiovascular Surgery. 2019; 48(1): 18-24.

(4) Saito A, Hirahara N, Motomura N, Miyata H, Takamoto S. Current Status of Cardiovascular Surgery in Japan: Analysis of Data from Japan Cardiovascular Surgery Database in 2015, 2016. Japanese Journal of Cardiovascular Surgery. 2019; 48(1): 6-10.

(5) Boer C, Meesters MI, Milojevic M, Benedetto U, Bolliger D, von Heymann C, et al. 2017 EACTS/EACTA Guidelines on patient blood management for adult cardiac surgery. Journal of Cardiothoracic and Vascular Anesthesia. 2018; 32(1): 88-120.

(6) Ferraris VA, Brown JR, Despotis GJ, Hammon JW, Reece TB, Saha SP, et al. 2011 Update to The Society of Thoracic Surgeons and the Society of Cardiovascular Anesthesiologists Blood Conservation Clinical Practice Guidelines**The International Consortium for Evidence Based Perfusion formally endorses these guidelines. The Annals of Thoracic Surgery. 2011; 91(3): 944-82.

(7) Murphy GS, Hessel EA, Groom RC, et al. Optimal perfusion during cardiopulmonary bypass: an evidence-based approach. Anesthesia & Analgesia. 2009; 108(5): 1394-417.

(8) Gravlee GP. Cardiopulmonary bypass: principles and practice. Lippincott Williams & Wilkins; 2008.

(9) Hall JE. Guyton and Hall Textbook of Medical Physiology. 14th ed. Philadelphia, PA: Elsevier; 2020.

(10) Yamaguchi A, Momose N. Jinko Shinpai Handbook 3rd Ed. Tokyo: ChugaiIgakusha; 2020 (in Japanese).

(11) Hilberath J, Thomas ME, Smith T, Jara C, Fitzgerald D, Wilusz K, et al. Blood volume measurement by hemodilution: association with valve disease and re-evaluation of the Allen Formula. Perfusion. 2015; 30(4): 305-11.

(12) Hasegawa T, Iba Y, Naraoka S, Nakajima T, Hashimoto S, Murohashi T, et al. Improvement of predicted hematocrit values after the initiation of cardiopulmonary bypass in cardiovascular surgery. Journal of Artificial Organs. 2021; 25:

1-8.
(13) Trowbridge, Cody, Stammers, Alfred, Klayman, Myra, Brindisi, Nicholas. A Novel Calculation to Estimate Blood Volume and Hematocrit During Bypass. J Extra Corpor Technol. 2008; 40(1): 61-4.
(14) Muraki R, Hiraoka A, Nagata K, Nakajima K, Oshita T, Arimichi M, et al. Novel method for estimating the total blood volume: the importance of adjustment using the ideal body weight and age for the accurate prediction of haemodilution during cardiopulmonary bypass. Interactive CardioVascular and Thoracic Surgery. 2018; 27(6): 802-7.
(15) Erpicum M, Dardenne N, Hans G, Larbuisson R, Defraigne JO. Prediction of the post-dilution hematocrit during cardiopulmonary bypass. Are new formulas needed? Perfusion. 2016; 31(6): 458-64.
(16) Hibiya M, Kamei T, Kubota S, et al. Study profile of the perfusion registry in Japan. Japanese Journal of Extra-Corporeal Technology. 2018; 45(1): 1-7.
(17) Du Bois D, Du Bois EF. A formula to estimate the approximate surface area if height and weight be known. Archives of Internal Medicine. 1916; 17(6): 863-71.
(18) Japan Society for the Study of Obesity. GUIDELINES FOR THE MANAGEMENT OF OBESITY DISEASE 2022. Tokyo: Life Science Publishing; 2022 (in Japanese).
(19) Shin DA, Lee JC, Shin H, Cho YJ, Kim HC. Point-of-care testing of plasma free hemoglobin and hematocrit for mechanical circulatory support. Scientific Reports. 2021; 11(1): 3788.
(20) Guyon I, Elisseeff A. An introduction to variable and feature selection. J Mach Learn Res. 2003; 3(null): 1157–1182.
(21) Jolliffe IT, Cadima J. Principal component analysis: a review and recent developments. Philosophical Transactions of the Royal Society A: Mathematical, Physical and Engineering Sciences. 2016; 374(2065): 20150202.
(22) Hornik K, Stinchcombe M, White H. Multilayer feedforward networks are universal approximators. Neural Networks. 1989; 2(5): 359-66.
(23) Marquardt DW. An Algorithm for Least-Squares Estimation of Nonlinear Parameters. Journal of the Society for Industrial and Applied Mathematics. 1963; 11(2): 431-41.
(24) Riedmiller M, Braun H. A direct adaptive method for faster backpropagation learning: the RPROP algorithm. In: IEEE International Conference on Neural Networks; 1993. p. 586-91 vol.1.
(25) Hoerl AE, Kennard RW. Ridge Regression: Biased Estimation for Nonorthogonal Problems. Technometrics. 1970; 12(1): 55-67.

After modification 12-1

P. 21

(1) Hirata Y, Hirahara N, Murakami A, Motomura N, Miyata H, Takamoto S. Current status of cardiovascular surgery in Japan: analysis of data from Japan cardiovascular surgery database in 2015, 2016. 1. congenital heart surgery. Jpn J Cardiovasc Surg. 2019; 48(1): 1-5 (in Japanese).
(2) Abe T, Nakano K, Hirahara N, Motomura N, Miyata H, Takamoto S, Current Status of cardiovascular surgery in Japan: analysis of data from Japan cardiovascular surgery database in 2015, 2016. 3-Valvular heart surgery. Jpn J Cardiovasc Surg. 2019; 48(1): 11-7 (in Japanese).
(3) Shimizu H, Hirahara N, Motomura N, Miyata H, Takamoto S. Current status of cardiovascular surgery in Japan: analysis of data from Japan cardiovascular surgery database in 2015, 2016. 4-Thoracic aortic surgery. Jpn J Cardiovasc

Surg. 2019; 48(1): 18-24 (in Japanese).

(4) Saito A, Hirahara N, Motomura N, Miyata H, Takamoto S. Current status of cardiovascular surgery in Japan: analysis of data from Japan cardiovascular surgery database in 2015, 2016. 2. Isolated Coronary Artery Bypass Surgery. 2-Isolated coronary artery bypass surgery. Jpn J Cardiovasc Surg. 2019; 48(1): 6-10 (in Japanese).

(5) Taniguchi FP, Martins AS. Hemodilution, kidney dysfunction and cardiac surgery. Einstein (Sao Paulo). 2009;7(1 Pt 1):103-7.

(6) Ranucci M, Conti D, Castelvecchio S, et al. Hematocrit on cardiopulmonary bypass and outcome after coronary surgery in nontransfused patients. Ann Thorac Surg. 2010; 89(1): 11-17.

(7) Karkouti K, Djaiani G, Borger MA, et al. Low hematocrit during cardiopulmonary bypass is associated with increased risk of perioperative stroke in cardiac surgery. Ann Thorac Surg. 2005; 80(4): 1381-1387.

(8) Tsui AKY, Dattani ND, Marsden PA, et al. Reassessing the risk of hemodilutional anemia: Some new pieces to an old puzzle. Can J Anaesth. 2010; 57(8): 779-791.

(9) Boer C, Meesters MI, Milojevic M et al. 2017 EACTS/EACTA Guidelines on patient blood management for adult cardiac surgery. J Cardiothorac Vasc Anesth. 2018; 32(1): 88-120.

(10) Ferraris VA, Brown JR, Despotis GJ et al. 2011 Update to The Society of Thoracic Surgeons and the Society of Cardiovascular Anesthesiologists Blood Conservation Clinical Practice Guidelines**The International Consortium for Evidence Based Perfusion formally endorses these guidelines. Ann Thorac Surg. 2011; 91(3): 944-982.

(11) Murphy GS, Hessel EA, Groom RC et al. Optimal perfusion during cardiopulmonary bypass: an evidence-based approach. Anesth Analg. 2009; 108(5): 1394-1417.

(12) Gravlee GP. Cardiopulmonary bypass: principles and practice. 3rd ed. Philadelphia, PA: Lippincott Williams & Wilkins; 2008:403-409.

(13) Hall JE. Guyton and Hall Textbook of Medical Physiology. 14th ed. Philadelphia, PA: Elsevier; 2020: 305-310.

(14) Sonoki T, Mushino T, Ueda Y et al., Use guidelines on red blood cell preparation based on scientific grounds (the revision third edition). Jpn J Transfusion Cell Therapy. 2024; 70(6): 579—596 (in Japanese).

(15) Hilberath J, Thomas ME, Smith T et al. Blood volume measurement by hemodilution: association with valve disease and re-evaluation of the Allen Formula. Perfusion. 2015; 30(4): 305-311.

(16) Hasegawa T, Iba Y, Naraoka S et al. Improvement of predicted hematocrit values after the initiation of cardiopulmonary bypass in cardiovascular surgery. J Artif Organs. 2021; 25: 1-8.

(17) Trowbridge C, Stammers A, Klayman M, Brindisi N. A Novel Calculation to Estimate Blood Volume and Hematocrit During Bypass. J Extra Corpor Technol. 2008; 40(1): 61-4.

(18) Muraki R, Hiraoka A, Nagata K et al. Novel method for estimating the total blood volume: the importance of adjustment using the ideal body weight and age for the accurate prediction of haemodilution during cardiopulmonary bypass. Interact Cardiovasc Thorac Surg. 2018; 27(6): 802-7.

(19) Erpicum M, Dardenne N, Hans G, Larbuisson R, Defraigne JO. Prediction of the post-dilution hematocrit during cardiopulmonary bypass. Are new formulas needed? Perfusion. 2016; 31(6): 458-464.

(20) Hibiya M, Kamei T, Kubota S et al. Study profile of the perfusion registry in Japan. Jpn J Extra Corpor Technol. 2018; 45(1): 1-7.

(21) Du Bois D, Du Bois EF. A formula to estimate the approximate surface area if height and weight be known. Arch Int

Med. 1916; 17(6): 863-871.

(22) Japan Society for the Study of Obesity. Guidelines for the management of obesity disease 2022. Tokyo: Life Science Publishing; 2022: 1-7 (in Japanese).

(23) Shin DA, Lee JC, Shin H, Cho YJ, Kim HC. Point-of-care testing of plasma free hemoglobin and hematocrit for mechanical circulatory support. Sci Rep. 2021; 11(1): 3788.

(24) Maharana K, Mondal S, Nemade B. A review: Data pre-processing and data augmentation techniques. Global Transitions Proceedings. 2022; 3(1): 91-99.

(25) Hancock JT, Khoshgoftaar TM. Survey on categorical data for neural networks. J Big Data. 2020; 7: 28.

(26) Guyon I, Elisseeff A. An introduction to variable and feature selection. J Mach Learn Res. 2003; 3: 1157–1182.

(27) Jolliffe IT, Cadima J. Principal component analysis: a review and recent developments. Philos Trans Royal Soc A: Math, Phys Eng Sci. 2016; 374(2065): 20150202.

(28) J.M. Bland, D.G. Altman, Comparing methods of measurement: why plotting difference against standard method is misleading, Lancet. 1995; 346(8982): 1085-1087.

(29) Bland JM, Altman DG. Measuring agreement in method comparison studies. Stat Methods Med Res. 1999; 8: 135–60.

(30) Marquardt DW. An Algorithm for Least-Squares Estimation of Nonlinear Parameters. J Soc Indust Appl Math. 1963; 11(2): 431-41.

(31) Riedmiller M, Braun H. A direct adaptive method for faster backpropagation learning: the RPROP algorithm. In: IEEE Int Conf Neural Netw; 1993; 1: 586-91.

(32) Hoerl AE, Kennard RW. Ridge regression: biased estimation for nonorthogonal problems. Technometrics. 1970; 12(1): 55-67.

[Reviewer 2]

Response to comments of **reviewer 2** on the paper "Estimation of Hemoglobin Concentration at the Initiation of Cardiopulmonary Bypass Using Support Vector Regression" reference ject250087

First of all, the authors thank the reviewer for their comments. The reviewer's concerns are addressed below.

●Comment (1)

In order to maximize the utility of the manuscript within the target publication, please consider adding to the discussion: How might a computationally intensive method such as this find it's way into the operating room?

Response (1)

Thank you for the suggestion. We have added a paragraph to the Discussion describing a practical pathway for clinical deployment. Model development and training are performed on a workstation or cloud environment due to computational requirements. Once trained, however, inference is lightweight and can be executed on standard devices (e.g., a laptop or smartphone), making in-the-OR use feasible. The model can run locally with low latency and without the need for specialized hardware. We also note that integration into perfusion workflows (e.g., as a simple calculator or as an EMR/perfusion-system plugin) and consideration of governance aspects (validation, monitoring, and data security) constitute part of our future work, which has been added to the Limitations section.

Before modification 1-1

P. 16

Therefore, Hb_{CPB} cannot be fully explained by body weight, priming volume, and preoperative Hb concentration alone, as suggested by conventional approaches. These findings highlight the influence of additional confounding variables, including age and comorbidities.

After modification 1-1

P. 15

Therefore, Hb_{CPB} cannot be fully explained by body weight, priming volume, and preoperative Hb concentration alone, as suggested by conventional approaches. At the same time, while models using PCs 1–17 showed better performance than the conventional formula, we cannot presently ascribe the improvement to specific components without dedicated ablation or feature-contribution analyses. These findings highlight the influence of additional confounding variables, including age and comorbidities. Although model development and training require computational resources (workstation- or cloud-based), inference is lightweight and can be executed on common devices (e.g., a standard laptop or smartphone) with low latency and no specialized hardware. This enables point-of-care use in the operating room as a simple calculator or as a module integrated into existing perfusion workflows.

Addition 1-2

P. 18

Limitations

Although inference is feasible on standard devices, clinical integration remains ongoing. Both EHR-based and device-based (perfusion console) deployments are feasible, but practical adoption will require: (A) interoperability with hospital systems and/or perfusion consoles, (B) a user interface suited to intraoperative workflow, (C) prospective validation with monitoring for model drift, and (D) security and access control consistent with institutional policies. We plan to evaluate these aspects and conduct prospective usability and safety assessments prior to routine operating-room adoption.

●Comment (2)

Could this be implemented within an EHR, or would it need to be added to one of the existing perfusion hardware devices (VIPER, etc.)?

Response (2)

Both deployment pathways are feasible. The model can be integrated within an EHR (e.g., as a calculator embedded in an order set, flowsheet, or CDS module) or on existing perfusion hardware (e.g., as a plug-in for devices such as VIPER). In both scenarios, model training is performed offline (workstation or cloud), while inference is lightweight and can run on standard hardware. We have added text clarifying these options and noted implementation and validation as part of future work in the Limitations section.

Before modification 2-1

P. 16

These findings highlight the influence of additional confounding variables, including age and comorbidities.

After modification 2-1

P. 16

These findings highlight the influence of additional confounding variables, including age and comorbidities.
Although model development and training require computational resources (workstation- or cloud-based), inference is lightweight and can be executed on common devices (e.g., a standard laptop or smartphone) with low latency and no specialized hardware. This enables point-of-care use in the operating room as a simple calculator or as a module integrated into existing perfusion workflows. Accordingly, the trained model can be delivered either (i) within the EHR as a point-of-care calculator or clinical decision support widget that auto-populates inputs from routinely collected pre-CPB data, or (ii) on perfusion hardware (e.g., as a vendor plug-in) to present predictions alongside pump parameters. After deployment, the model can operate offline, and input variables can be populated automatically from routine pre-CPB data, minimizing manual entry and cognitive load.

Addition 2-2

P. 18

Limitations

While inference is feasible on standard devices, clinical integration remains ongoing work. Both EHR-based and device-based (perfusion console) deployments are feasible, but practical adoption will require (A) interoperability with hospital systems and/or perfusion consoles, (B) a user interface suited to intraoperative workflow, (C) prospective validation with monitoring for model drift, and (D) security and access control consistent with institutional policies. We plan to evaluate these aspects and conduct prospective usability and safety assessments prior to routine operating-room adoption.

●Comment (3)

The R2 value of the best performing method (while notably better than existing common methods) seemed somewhat modest - please add this to the discussion, along with references to comparable tools and their performance.

Response (3)

Thank you for this observation. We note that agreement is more appropriately assessed using Bland–Altman (BA) analysis rather than correlation alone. In our data, BA analysis demonstrates smaller bias and narrower limits of agreement for the novel methods (Fig. 3(a)–(c)) compared with the conventional formulas (Fig. 3(d)–(e)), indicating improved agreement despite moderate R^2 values. We have cited BA as a complementary evaluation tool and included references to the seminal methodology papers by Bland and Altman (1995, 1999). The Discussion has been revised accordingly.

Addition 3-1

P. 17

Overall, SVR and MLP, which perform nonlinear function estimation and embed variable selection within the model, outperformed linear models, including conventional approaches, in predicting outcomes from high-dimensional medical data.

Although the best-performing method yielded a modest R^2, agreement relevant to bedside use is better captured by Bland–Altman analysis (28, 29): the new methods demonstrated minimal bias and narrower limits of agreement than the conventional formulas (Figure 5), indicating improved agreement despite a moderate R^2 compared with the previous methods. Finally, while models using multiple principal components outperformed the conventional formula, we cannot presently ascribe the improvement to specific components without dedicated ablation or feature-contribution analyses; this is noted as a limitation and will be addressed in future work.

Addition 3-2

P. 24

(28) J.M. Bland, D.G. Altman, Comparing methods of measurement: why plotting difference against standard method is misleading, Lancet. 1995; 346(8982). 1085-1087.

(29) Bland JM, Altman DG. Measuring agreement in method comparison studies. Stat Methods Med Res. 1999; 8: 135–60.

●Comment (4)

Also please consider adding a discussion of the costs and benefits of implementing a computationally intensive algorithm such as this. We can see that the performance is somewhat better with your approach, however implementing it would involve considerable software programming expense - how large of a benefit might one expect for patients and cardiac programs by engaging in such an expense?

Response (4)

Thank you for this important point. We have added a paragraph to the Discussion outlining both costs and benefits. Model development and training are computationally intensive but can be performed cost-effectively on a workstation or cloud platform using widely available open-source tools. Once trained, inference is lightweight and can run on standard hospital devices (e.g., laptop or tablet) without specialized hardware, keeping deployment costs low. The anticipated clinical benefits include more accurate estimation of Hb_{CPB} at pump initiation, supporting tighter transfusion management and potentially reducing unnecessary transfusions and anemia-related risks, thereby improving care quality and workflow consistency. We also note that prospective evaluation of clinical impact and a formal cost-effectiveness analysis are planned as part of future work.

Addition 4-1

P. 17

Model development and training require computational resources; these activities can be conducted cost-effectively on a workstation or in the cloud using open-source machine-learning frameworks. After training, inference is lightweight, runs on commodity devices without accelerators, and can be embedded in existing EHR or perfusion-system workflows with minimal latency. From a clinical perspective, more accurate prediction of Hb_{CPB} at CPB initiation supports optimized transfusion strategies—reducing the likelihood of both under- and over-transfusion—and may help lower hemodilution-related risks while standardizing practice across teams. We therefore view the cost–benefit balance as favorable, while acknowledging that prospective evaluation of clinical outcomes and a formal cost-effectiveness analysis are warranted in future work.

Estimation of Hemoglobin Concentration at the Initiation of Cardiopulmonary Bypass Using Support Vector Regression

Harutoyo Hirano[1, *], PhD, Shun Takahashi[2, *], Tetsuya Kamei[3], PhD, Makoto Hibiya[4, †], PhD

1. Department of Medical Equipment Engineering, Clinical and Educational Collaboration Unit, Faculty of Medical Sciences, Fujita Health University, Toyoake, Aichi, Japan

2. Department of Biomedical Engineering, Graduate School of Medical Science, Fujita Health University, Toyoake, Aichi, Japan

3. Fundamental Education Department, Faculty of Medical Sciences, Fujita Health University, Toyoake, Aichi, Japan

4. Department of Clinical Engineering, Clinical and Educational Collaboration Unit, Faculty of Medical Sciences, Fujita Health University, Toyoake, Aichi, Japan

* *These two authors contributed equally to this work.*

† *Corresponding author*: mhibiya@fujita-hu.ac.jp

Estimation of Hemoglobin Concentration at the Initiation of Cardiopulmonary Bypass Using Support Vector Regression

Keywords

hemoglobin, support vector regression, cardiopulmonary bypass, machine learning, hemodilution

Abstract

Background: Hemodilution during cardiopulmonary bypass (CPB) is a standard perfusion strategy used to reduce blood viscosity and enhance microcirculatory flow. The hemodilution rate, expressed as hemoglobin (Hb) concentration, is a key control index in CPB and is currently estimated from total blood volume (TBV). The objective of this study was to propose a novel formula to accurately predict Hb concentration at the initiation of CPB (Hb_{CPB}) by incorporating circulating blood volume, laboratory data, physical measurements, and patient history.

Methods: We retrospectively analyzed 577 adult patients who underwent elective CPB at Fujita Health University Hospital from January 2016 to December 2020. Thirty-six preoperative variables—including demographics, laboratory data, circuit parameters, and indices such as TBV and ideal weight—were standardized. Categorical variables underwent one-hot encoding. We compared generalized linear models (GLM), support vector regression (SVR), and multilayer perceptron (MLP). Model performance was evaluated using the coefficient of determination (R^2), mean squared error (MSE), and Bland–Altman analysis (bias and 95% limits of agreement [LoA]). Predictions from two

Reviewer1 6-1

Reviewer1 7-1

conventional TBV-based formulas were used as benchmarks.

Results: Of 993 screened cases, 577 met inclusion criteria (447 males, mean age 66.8 ± 11.7 years; 130 females, 69.5 ± 10.6 years). SVR on standardized predictors achieved the highest accuracy (R^2 = 0.498, MSE = 0.517), outperforming GLM (R^2 = 0.429, MSE = 0.797) and MLP (R^2 = 0.332, MSE = 0.669). Conventional formulas showed lower performance (R^2 = 0.325, MSE ≥ 1.48). Bland–Altman analysis for SVR demonstrated minimal bias (–0.0028 g/dL) and narrower LoA (–1.42 to 1.41 g/dL) than conventional methods (bias –1.33 g/dL; LoA –3.49 to 0.83 g/dL).

Conclusion: These findings suggest that an SVR-based model improves prediction of Hb_{CPB} over conventional approaches, supporting optimized transfusion management and reduced hemodilution-related risks.

Introduction

Japan's population is aging rapidly, and the proportion of elderly patients undergoing cardiac surgery with cardiopulmonary bypass (CPB) has steadily increased over the past decade (1–4). As this trend is expected to continue, developing appropriate CPB technologies for older patients has become imperative. Hemodilution during CPB is a standard perfusion strategy used to reduce blood viscosity and enhance microcirculatory flow (5). However, anemia resulting from hemodilution may cause ischemic organ injury, increase mortality, and elevate stroke risk (6, 7, 8). Current guidelines recommend maintaining hematocrit (Ht) levels ≥ 21% and/or hemoglobin (Hb) concentrations ≥ 7.0 g/dL during CPB to minimize hemodilution-related complications (9, 10, 11). To assess the hemodilution rate, total blood volume (TBV) is estimated using body weight in kilograms (kg). TBV estimates are typically set at 70 mL/kg for American adult males, 65 mL/kg for females (12, 13), and 80 mL/kg for Japanese adults (14). This method is commonly applied to all adults, regardless of age. However, several studies have shown discrepancies between predicted post-dilution Ht or Hb values and actual Hb concentrations at the initiation of CPB (Hb_{CPB}) (15–17). Revised formulas incorporating sex and age have been proposed to improve TBV estimates (18). Nonetheless, these methods often lack applicability to older patients, as they do not adequately account for age-related TBV decline (19).

This study aims to develop and propose a novel formula to predict Hb_{CPB} more accurately by

incorporating TBV, laboratory data, physical measurements, and clinical history.

Materials and Methods

Clinical data

This study analyzed data that were prepared to register in the Perfusion Database maintained by the Japanese Society of Extra-Corporeal Technology in Medicine (JaSECT) for patients who underwent cardiac surgery with CPB at Fujita Health University Hospital between January 1, 2016, and December 31, 2020. Only elective cases were included. Patients with congenital heart disease or those who underwent repeat surgeries were excluded to avoid duplicate entries, particularly in preoperative background data. Additionally, cases involving blood priming or with hemoglobin (Hb) concentrations below 7 g/dL at CPB initiation were excluded. Details of the data cleaning process are shown in Figure 1. The JaSECT Perfusion Database collects data across six domains: patient demographics; circuit and priming fluid details; CPB parameters; fluid volume input and output management; laboratory data and outcomes. These domains consist of 84 multiple-choice items and 159 numeric variables, totaling 243 parameters (20). From in-hospital data for this database, we extracted 35 pre-CPB parameters along with $\mathrm{Hb}_{\mathrm{CPB}}$ for model development, as described in the following section.

- **Demographic and clinical variables**: sex; age at surgery; surgical procedure; height; weight;

left ventricular ejection fraction; and risk factors, including congestive heart failure, chronic respiratory disease, smoking history, diabetes mellitus, arrhythmia, hypertension, dyslipidemia, cardiovascular or extracardiac vascular disease, cerebrovascular disease, renal dysfunction, and chronic dialysis.

- **Blood laboratory data obtained by the time of admission to the operating room**: glucose (mg/dL); potassium (mEq/L); lactate (mg/dL); creatinine (mg/dL); Hb (g/dL); results of arterial blood gas analysis (pH, PaO_2(mmHg), $PaCO_2$(mmHg), HCO_3^-(mEq/L)) and activated clotting time (sec)
- **Variables described the CPB circuit configuration**: biocompatible coating part; planned priming volume (Static circuit volume); and priming fluid composition.
- **Variables obtained from formulas using collected data**: ideal body weight; TBV; body mass index (BMI); obesity classification; and body surface area (BSA).

BMI, ideal body weight (BW_i) (18), TBV (11) and BSA (21) were calculated as follows (Equations (i)–(iv)):

Reviewer1 3-1

$$\mathrm{BMI} = \frac{w}{h^2}, \quad \text{(i)}$$

$$\mathrm{BW_i} = 22h^2, \quad \text{(ii)}$$

$$\mathrm{TBV} = 80w, \quad \text{(iii)}$$

$$\mathrm{BSA} = 0.7184 \times 10^{-4} \times h^{0.725} \times w^{0.425}, \quad \text{(iv)}$$

where w is the body weight (kg) and h is the height (m).

Obesity was classified according to the Japanese Society for the Study of Obesity Guidelines (22) as follows: underweight (BMI < 18.5 kg/m^2), normal weight (18.5 ≤ BMI < 25 kg/m^2), obesity class I (25 ≤ BMI < 30 kg/m^2), class II (30 ≤ BMI < 35 kg/m^2), class III (35 ≤ BMI < 40 kg/m^2), and class IV (BMI ≥ 40 kg/m^2). Hematocrit (Ht) values measured before and at CPB initiation were converted to Hb concentrations using the equation: $\mathrm{Ht} \approx 3 \times \mathrm{Hb}$ (23).

Analysis protocol

Preprocessing of eligible Clinical Data

The 35 parameters described in the previous section were considered candidate explanatory variables for estimating $\mathrm{Hb}_{\mathrm{CPB}}$. One-hot encoding was applied to 15 categorical variables (e.g., sex, type of surgery, and presence of comorbidities), and z-score standardization was applied to 20 continuous variables (e.g., laboratory data) (24, 25). The interactions among variables, and between each variable and hemoglobin concentration, remain unknown. In general, including variables with low or no relevance to the target variable may impair the generalizability of a predictive model and lead to overfitting. It is therefore advisable to limit explanatory variables to those that carry significant information about the outcome (26). However, this restriction may exclude potentially informative features. To address this, we prepared two datasets for analysis: the full standardized dataset and a

Reviewer1 10-1

dimensionally reduced dataset, described below.

Principal Component Analysis (PCA) (27) was applied to the standardized explanatory matrix $\mathbf{X} \in \mathbb{R}^{N\times P}$ (where N is the number of subjects and P is the number of variables) to mitigate multicollinearity. Eigenvalue decomposition was performed on the covariance matrix $\Sigma = \frac{1}{N-1}, \mathbf{X}^{\mathrm{T}}\mathbf{X}$, and the smallest number of principal components K was selected such that the cumulative contribution of the eigenvalues $\lambda_k{}_{k=1}^{P}$ exceeded 90 %. Next, the principal component score matrix $\mathbf{P} = [\mathbf{t}_1, \ldots, \mathbf{t}_K,] = \mathbf{X}[\mathbf{v}_1, \ldots, \mathbf{v}_K] \in \mathbb{R}^{N\times K}$ was calculated using the principal component vector $v_k{}_{k=1}^{K}$. After PCA, $\mathbf{P}$ was used as the explanatory variable for the subsequent model training.

Reviewer1 2-1

Linear model for predicting hemoglobin concentration at CPB initiation

Conventional methods for estimating $\mathrm{Hb}_{\mathrm{CPB}}$ (17–19) are essentially linear models that incorporate a limited set of patient and circuit factors, such as priming volume. We first evaluated whether a linear approach would be adequate for our dataset. To do so, we fit a generalized linear model (GLM) using routinely available pre-CPB variables, including body size indices, laboratory values, and circuit settings. The GLM assumes that $\mathrm{Hb}_{\mathrm{CPB}}$ varies in approximate proportion to changes in these inputs. Model performance was assessed using the coefficient of determination (R^2) and mean squared error (MSE). The explicit GLM equation and estimation procedures are provided in Supplementary Equation (S-i).

Nonlinear model for predicting hemoglobin concentration at CPB initiation

Because clinical data often contain nonlinear relationships and interactions that linear models may not capture, we also evaluated two standard nonlinear approaches: Support Vector Regression (SVR) and a Multilayer Perceptron (MLP).

SVR can model curved relationships between the inputs and Hb_{CPB} without the need to specify functional forms. We used a widely adopted SVR implementation and tuned its hyperparameters by cross-validation to reduce overfitting; further details are provided in the Supplement (equations s-ii, iii). The MLP is a simple neural-network model that learns patterns by stacking a small number of layers. We compared several compact architectures and training configurations and selected the model that performed best in cross-validation. Training details (architecture and stopping criteria) are summarized in the Supplement (equation s-iv).

For some analyses, we also used a compressed set of input variables derived from principal component analysis to reduce redundancy among predictors. We retained the smallest number of components that preserved approximately 90% of the total variance. Technical details are provided in Supplement S2.

Model training, validation, and reporting

For all models, we standardized inputs when appropriate, tuned model settings by cross-validation, and summarized performance using $R^2$and MSE. Because correlation-based indices do not measure exact agreement, we also evaluated agreement between predicted and measured $\mathrm{Hb}_{\mathrm{CPB}}$ with Bland–Altman analysis (bias and 95% limits of agreement).

Software and reproducibility

Analyses were performed with commonly used, off-the-shelf software (e.g., MATLAB equivalents or open-source alternatives). Parameter settings and code snippets sufficient for reproduction are listed in the Supplement.

Evaluation of the proposed method

To evaluate the performance of the trained models, predictions on the validation and hold-out test sets were computed and compared against the reference values of $\mathrm{Hb}_{\mathrm{CPB}}$. As this is a regression task, three metrics were used to quantify prediction accuracy: MSE, mean absolute error, and the coefficient of determination (R^2). In addition, Bland–Altman analysis was performed to further examine the agreement between predicted and measured hemoglobin concentrations. From this analysis, the mean difference (bias) and 95% limits of agreement (LoA), defined as ±1.96 times the standard deviation of

the differences, were calculated.

To benchmark our method against conventional prediction models, the same clinical dataset was fitted using the standard hematocrit-based prediction formula (18), which is expressed as:

$$\mathrm{Ht_{CPB}} = \mathrm{Ht_{beforeCPB}} \times \left(1 - \frac{\mathrm{PV}}{\mathrm{PV} + \mathrm{TBV}}\right), \quad \text{(v)}$$

Reviewer1 3-2

where $\mathrm{Ht_{CPB}}$ is the hematocrit value under CPB, $\mathrm{Ht_{beforeCPB}}$ is the hematocrit value before CPB, PV is Priming Volume. TBV was substituted from two approaches: Equation (iii) (19) and the following equation (18):

$$\mathrm{TBV} = \begin{cases} 70 \times \mathrm{BW} & (\mathrm{Age} < 65) \\ 60 \times BW & (\mathrm{Age} \geq 65) \end{cases}, \quad \text{(vi)}$$

Estimated Hb concentrations based on Equation (v) and their Bland–Altman statistics, mean difference, and 95 % LoA, were compared with those obtained for our approach.

Results

Data from 577 patients, including 447 males (mean age 66.1 ± 11.8 years) and 130 females (mean age 69.5 ± 10.6 years), were included in the analysis. Subject characteristics are summarized in Table 1. In terms of obesity classification, 31 patients (5.4%) were underweight, 361 (62.6%) were standard weight, 146 (25.3%) were classified as obese class I, 33 (5.7%) as class II, 5 (0.8%) as class III, and 1 (0.2%) as class IV. The surgical procedures included coronary artery bypass grafting (CABG) in 149 patients (25.8%), valve surgery in 215 (37.3%), combined CABG and valve procedures in 67 (11.6%),

combined CABG and other procedures in 27 (4.7%), aortic surgery in 91 (15.8%), and other procedures in 28 (4.8%). Regarding biopassive coating, it was absent in 2 patients (0.3%), applied to limited components in 34 (5.9%), applied to all components except the cannulae in 484 (84.0%), and applied tip-to-tip in 57 (9.8%). The main priming solution was bicarbonate Ringer's in 540 patients (93.6%). Other solutions included saline in 17 (3.0%), lactated Ringer's in 2 (0.3%), acetate Ringer's in 3 (0.5%), starch or dextran in 3 (0.5%), and other crystalloid-only solutions in 12 (2.1%). A centrifugal pump was employed in all cases.

Figure 2 shows the scree plot of the principal components derived from PCA of the predictor matrix $\mathbf{X} \in \mathbb{R}^{N \times P}$, which comprises z-score standardized continuous variables and one-hot encoded categorical variables. From this plot, it was confirmed that 17 components were required to reach a cumulative explained variance of 90%. Figure 3 illustrates the five variables with the highest absolute loadings for each principal component. These results indicate that body weight was captured primarily by PC1, priming volume (static circuit volume) by PCs 5, 7, 9, and 11, and preoperative hemoglobin concentration by PCs 5, 8, 9, 12, 14, and 16. Table 2 presents the results of the generalized linear model fitted to the PCA-transformed predictors. The analysis revealed that intraoperative $\mathrm{Hb}_{\mathrm{CPB}}$ was primarily determined by six principal components: PC1, PC2, PC5, PC8, PC12, and PC14.

Figure 4 shows the comparison between measured $\mathrm{Hb}_{\mathrm{CPB}}$ and predicted values based on pre-CPB variables, while Table 3 summarizes model performance indices. For each scatter plot in Figure

Reviewer1 5-1

4, the ordinary least-squares regression slopes and y-intercepts—where better estimation is reflected by a slope close to 1 and a y-intercept close to 0—are displayed. The slopes and intercepts (panels a–e) are as follows: (a) slope = 1.00, intercept = 4.00×10^{-5}; (b) slope = 1.22, intercept = −1.88; (c) slope = 0.92, intercept = 0.68; (d) slope = 0.44, intercept = 4.18; (e) slope = 0.48, intercept = 4.13. A GLM fitted to the standardized predictor matrix $\mathbf{X} \in \mathbb{R}^{N \times P}$ achieved a coefficient of determination of $R^2_{\mathrm{GLM}} = 0.429$, adjusted $R^2_{\mathrm{GLM}} = 0.369$, and $\mathrm{MSE}_{\mathrm{GLM}} = 0.797$. However, multicollinearity in the input matrix was confirmed, resulting in a lack of full rank. Applying the same GLM to PCA-transformed predictors $\mathbf{X}_{\mathrm{PCA}} \in \mathbb{R}^{N \times P_{\mathrm{PCA}}}$ yielded $R^2_{\mathrm{PCR}} = 0.371$ (adjusted $R^2_{\mathrm{PCR}} = 0.352$) and $\mathrm{MSE}_{\mathrm{PCR}} = 0.808$. SVR on $\mathbf{X}$ with optimized hyperparameters $C = 2.279$, $\gamma = 16.81$, and $\varepsilon = 0.594$ yielded $R^2_{\mathrm{SVR}} = 0.498$ and 10-fold CV $\mathrm{MSE}_{\mathrm{SVR}} = 0.517$, outperforming the GLM. When SVR was applied to $\mathbf{X}_{\mathrm{PCA}}$ with $C = 1.662$, $\gamma = 14.28$, and $\varepsilon = 0.0084$, performance decreased to $R^2_{\mathrm{SVR_{PCA}}} = 0.39$ and CV $\mathrm{MSE}_{\mathrm{SVR_{PCA}}} = 0.52$. The MLP model, tuned via nested 5-fold CV, selected one hidden-layer architecture of 4 neurons, with Resilient Backpropagation, a learning rate of 10^{-2}, and early stopping tolerance of 10. On $\mathbf{X}$, this configuration yielded $R^2_{\mathrm{MLP}} = 0.332 \pm 0.033$ and $\mathrm{MSE}_{\mathrm{MLP}} = 0.669 \pm 0.086$. When applied to $\mathbf{X}_{\mathrm{PCA}}$, the MLP achieved $R^2 = 0.352 \pm 0.054$ and MSE = 0.646 ± 0.068. The coefficients of determination from both MLP configurations were lower than those from SVR. Previously published $\mathrm{Hb}_{\mathrm{CPB}}$ prediction formulas yielded $R^2 = 0.3225$, MSE = 2.98 based on (19), and $R^2 = 0.3245$, MSE = 1.48 based on (18), both substantially lower than SVR

performance.

Figure 5 displays the Bland–Altman analysis results. The bias between predicted and measured GLM values was -5×10^{-7} g/dL (95% CI: -0.0654 to 0.0654 g/dL), with 95% LoA of [–1.57 g/dL, 1.57 g/dL]. For SVR, the bias was –0.0028g/dL (95% CI: -0.0619 to 0.0562g/dL) with LoA of [–1.41 g/dL, 1.41 g/dL]. For MLP, the bias was –0.029 g/dL (95% CI: -0.0963 to 0.0375g/dL), and LoA was [–1.63 g/dL, 1.57 g/dL]. In contrast, the conventional methods had a bias of –1.33 g/dL (95% CI: –1.41 to –1.24 g/dL) and LoA of [–3.49 g/dL, 0.831 g/dL] for the reference (11) and a bias of –0.64 g/dL (95% CI: –0.72 to –0.555 g/dL) and LoA of [–2.67g/dL, 1.39g/dL] for the Equation (v), respectively. The 95% CI for bias did not include zero, indicating systematic error. In comparison, CIs from GLM, SVR, and MLP included zero, suggesting no statistically significant bias and the absence of systematic error. Biases between measured and predicted $\mathrm{Hb}_{\mathrm{CPB}}$ from GLM, SVR, and MLP were not statistically significant (GLM: $p = 1.000, d = -6.5 \times 10^{-7}$; SVR: $p = 0.926, d = -0.004$; MLP: $p = 0.389, d = -0.036$). Conversely, biases from conventional models were confirmed (reference (11): $p < 0.01, d = -1.21$; Equation (v): $p < 0.01, d = -0.617$).

Reviewer1 11-1

Reviewer1 3-3

Discussion

The GLM demonstrated moderate goodness-of-it despite the multicollinearity present in the input parameter matrix $\mathbf{X} \in \mathbb{R}^{N \times P}$. In contrast, implementing PCR resulted in reduced model performance

across all evaluation metrics compared with the GLM. In PCR, dimensionality reduction is driven solely by the variance structure of the predictor matrix; therefore, principal components that explain substantial variance but have limited correlation with the response variable may still be retained as leading components. In this study, the first 17 principal components were adopted, collectively accounting for 90% cumulative explained variance in the predictor matrix. While this approach preserved most of the predictor information, it may have failed to isolate features most relevant to Hb_{CPB}. Furthermore, the first principal component accounted for more than 20% of the total variance, and PC1 and PC2 were primarily composed of weight, height, TBV, BSA, BMI, ideal weight, and obesity measures, supporting the interpretation that TBV-related factors remain central to Hb_{CPB} estimation. As a result, the PCR model may not have adequately captured the most predictive features of Hb_{CPB}, likely contributing to its reduced performance, as reflected in the lower coefficient of determination and higher MSE compared with the GLM using the full predictor set. Traditional predictors used to estimate Hb_{CPB}—including body weight, priming volume (static circuit volume), and preoperative Hb concentration—were embedded within the principal components retained by PCR and were selected as input features for both the SVR and MLP models. Nevertheless, several of the principal components used in Hb_{CPB} prediction did not primarily reflect these conventional parameters. Therefore, Hb_{CPB} cannot be fully explained by body weight, priming volume, and preoperative Hb concentration alone, as suggested by conventional approaches. At the same time,

Reviewer1 4-2

Reviewer2 1-1

while models using PCs 1–17 showed better performance than the conventional formula, we cannot presently ascribe the improvement to specific components without dedicated ablation or feature-contribution analyses. These findings highlight the influence of additional confounding variables, including age and comorbidities.

Although model development and training require computational resources (workstation- or cloud-based), inference is lightweight and can be executed on common devices (e.g., a standard laptop or smartphone) with low latency and no specialized hardware. This enables point-of-care use in the operating room as a simple calculator or as a module integrated into existing perfusion workflows. Accordingly, the trained model can be delivered either (i) within the EHR as a point-

Reviewer2 2-1

of-care calculator or clinical decision support widget that auto-populates inputs from routinely collected pre-CPB data, or (ii) on perfusion hardware (e.g., as a vendor plug-in) to present predictions alongside pump parameters. After deployment, the model can operate offline, with input variables populated automatically from routine pre-CPB data, minimizing manual entry and cognitive load.

Among the nonlinear models, SVR demonstrated a higher coefficient of determination and lower MSE compared with both the GLM and PCR, indicating that SVR had superior predictive power. In contrast, applying PCA prior to SVR led to a decreased coefficient of determination, likely due to the exclusion of Hb_{CPB}-related features during the PCA process, as these were among the bottom 10% of

principal components that were subsequently discarded. The MLP model, incorporating Levenberg–Marquardt–based parameter optimization and early stopping, achieved stable training. When applied to the standardized predictor matrix, MLP showed slightly lower performance than SVR but still achieved a moderate goodness-of-fit. Overall, SVR and MLP, which perform nonlinear function estimation and embed variable selection within the model, outperformed linear models, including conventional approaches, in predicting outcomes from high-dimensional medical data.

Although the best-performing method yielded a modest R^2, agreement relevant to bedside use Reviewer2 3-1
is better captured by Bland–Altman analysis (28, 29): the new methods demonstrated minimal bias and narrower limits of agreement than the conventional formulas (Figure 5), indicating improved agreement despite a moderate R^2 compared with previous methods. Finally, while models using multiple principal components outperformed the conventional formula, we cannot presently ascribe the improvement to specific components without dedicated ablation or feature-contribution analyses; this is noted as a limitation and will be addressed in future work.

Model development and training require computational resources; these activities can be Reviewer2 4-1
conducted cost-effectively on a workstation or in the cloud using open-source machine-learning frameworks. After training, inference is lightweight, runs on commodity devices without accelerators, and can be embedded in existing EHR or perfusion-system workflows with minimal latency. From a clinical perspective, more accurate prediction of Hb_{CPB} at CPB initiation supports optimized

transfusion strategies—reducing the likelihood of both under- and over-transfusion—and may help lower hemodilution-related risks while standardizing practice across teams. We therefore view the cost–benefit balance as favorable, while acknowledging that prospective evaluation of clinical outcomes and a formal cost-effectiveness analysis are warranted in future work.

Limitations

While the proposed model [illegible] outperformed the conventional formula, we cannot, at present, attribute this improvement to specific principal components without dedicated ablation or feature-contribution analyses. We acknowledge this as a limitation and plan to investigate the contribution of individual components and underlying variables in future work.

Reviewer1 4-3

Although inference is feasible on standard devices, clinical integration remains ongoing. Both EHR-based and device-based (perfusion console) deployments are feasible, but practical adoption will require: (A) interoperability with hospital systems and/or perfusion consoles, (B) a user interface suited to intraoperative workflow, (C) prospective validation with monitoring for model drift, and (D) security and access control consistent with institutional policies. We plan to evaluate these aspects and conduct prospective usability and safety assessments prior to routine operating-room adoption.

Reviewer2 1-2, 2-2

Funding

The authors received no funding to complete this research.

Conflict of Interest

The authors declare no conflict of interest.

Data Availability

Data available upon request from the corresponding author.

Author Contributions

H. H. contributed to the conceptualization and design of the study, performed data analysis, drafted the initial manuscript, and participated in the review and revision of the final version. S. T. conducted statistical analysis, contributed to data interpretation, and assisted in drafting the manuscript. T.K. participated in data analysis and provided a critical review of the manuscript. M. H. contributed to the study's conceptualization and design, provided overall supervision, and critically reviewed and revised the manuscript. All authors read and approved the final manuscript.

Ethics Approval

This study was approved by the Ethics Review Committee of Fujita Health University (Approval No. HM21-381).

Acknowledgement

The authors express their sincere gratitude to Tomoaki Yamashiro, Yusuke Nakamura, and the Clinical Engineering Department staff at Fujita Health University Hospital for their meticulous efforts in data collection.

References

(1) Hirata Y, Hirahara N, Murakami A, Motomura N, Miyata H, Takamoto S. Current status of cardiovascular surgery in Japan: analysis of data from Japan cardiovascular surgery database in 2015, 2016. 1. congenital heart surgery. Jpn J Cardiovasc Surg. 2019; 48(1): 1-5 (in Japanese).

(2) Abe T, Nakano K, Hirahara N, Motomura N, Miyata H, Takamoto S, Current Status of cardiovascular surgery in Japan: analysis of data from Japan cardiovascular surgery database in 2015, 2016. 3-Valvular heart surgery. Jpn J Cardiovasc Surg. 2019; 48(1): 11-7 (in Japanese).

(3) Shimizu H, Hirahara N, Motomura N, Miyata H, Takamoto S. Current status of cardiovascular surgery in Japan: analysis of data from Japan cardiovascular surgery database in 2015, 2016. 4-Thoracic aortic surgery. Jpn J Cardiovasc Surg. 2019; 48(1): 18-24 (in Japanese).

(4) Saito A, Hirahara N, Motomura N, Miyata H, Takamoto S. Current status of cardiovascular surgery in Japan: analysis of data from Japan cardiovascular surgery database in 2015, 2016. 2. Isolated Coronary Artery Bypass Surgery. 2-Isolated coronary artery bypass surgery. Jpn J Cardiovasc Surg. 2019; 48(1): 6-10 (in Japanese).

(5) Taniguchi FP, Martins AS. Hemodilution, kidney dysfunction and cardiac surgery. Einstein (Sao Paulo). 2009;7(1 Pt 1):103-7.

(6) Ranucci M, Conti D, Castelvecchio S, et al. Hematocrit on cardiopulmonary bypass and outcome after coronary surgery in nontransfused patients. Ann Thorac Surg. 2010; 89(1): 11-17.

Reviewer1 12-1

Reviewer1 8-2

Reviewer1 9-2

(7) Karkouti K, Djaiani G, Borger MA, et al. Low hematocrit during cardiopulmonary bypass is associated with increased risk of perioperative stroke in cardiac surgery. Ann Thorac Surg. 2005; 80(4): 1381-1387.

(8) Tsui AKY, Dattani ND, Marsden PA, et al. Reassessing the risk of hemodilutional anemia: Some new pieces to an old puzzle. Can J Anaesth. 2010; 57(8): 779-791.

(9) Boer C, Meesters MI, Milojevic M et al. 2017 EACTS/EACTA Guidelines on patient blood management for adult cardiac surgery. J Cardiothorac Vasc Anesth. 2018; 32(1): 88-120.

(10) Ferraris VA, Brown JR, Despotis GJ et al. 2011 Update to The Society of Thoracic Surgeons and the Society of Cardiovascular Anesthesiologists Blood Conservation Clinical Practice Guidelines**The International Consortium for Evidence Based Perfusion formally endorses these guidelines. Ann Thorac Surg. 2011; 91(3): 944-982.

(11) Murphy GS, Hessel EA, Groom RC et al. Optimal perfusion during cardiopulmonary bypass: an evidence-based approach. Anesth Analg. 2009; 108(5): 1394-1417.

(12) Gravlee GP. Cardiopulmonary bypass: principles and practice. 3rd ed. Philadelphia, PA: Lippincott Williams & Wilkins; 2008: 416-417.

(13) Hall JE. Guyton and Hall Textbook of Medical Physiology. 14th ed. Philadelphia, PA: Elsevier; 2020: 305-310.

(14) Sonoki T, Mushino T, Ueda Y et al., Use guidelines on red blood cell preparation based

on scientific grounds (the revision third edition). Jpn J Transfusion Cell Therapy. 2024; 70(6): 579—596 (in Japanese).

(15)Hilberath J, Thomas ME, Smith T et al. Blood volume measurement by hemodilution: association with valve disease and re-evaluation of the Allen Formula. Perfusion. 2015; 30(4): 305-311.

(16)Hasegawa T, Iba Y, Naraoka S et al. Improvement of predicted hematocrit values after the initiation of cardiopulmonary bypass in cardiovascular surgery. J Artif Organs. 2021; 25: 1-8.

(17)Trowbridge C, Stammers A, Klayman M, Brindisi N. A Novel Calculation to Estimate Blood Volume and Hematocrit During Bypass. J Extra Corpor Technol. 2008; 40(1): 61-4.

(18)Muraki R, Hiraoka A, Nagata K et al. Novel method for estimating the total blood volume: the importance of adjustment using the ideal body weight and age for the accurate prediction of haemodilution during cardiopulmonary bypass. Interact Cardiovasc Thorac Surg. 2018; 27(6): 802-7.

(19)Erpicum M, Dardenne N, Hans G, Larbuisson R, Defraigne JO. Prediction of the post-dilution hematocrit during cardiopulmonary bypass. Are new formulas needed? Perfusion. 2016; 31(6): 458-464.

(20)Hibiya M, Kamei T, Kubota S et al. Study profile of the perfusion registry in Japan. Jpn J Extra Corpor Technol. 2018; 45(1): 1-7.

(21)Du Bois D, Du Bois EF. A formula to estimate the approximate surface area if height and weight

be known. Arch Int Med. 1916; 17(6): 863-871.

(22)Japan Society for the Study of Obesity. Guidelines for the management of obesity disease 2022. Tokyo: Life Science Publishing; 2022: 1-7 (in Japanese).

(23)Shin DA, Lee JC, Shin H, Cho YJ, Kim HC. Point-of-care testing of plasma free hemoglobin and hematocrit for mechanical circulatory support. Sci Rep. 2021; 11(1): 3788.

Reviewer1 10-2

(24)Maharana K, Mondal S, Nemade B. A review: Data pre-processing and data augmentation techniques. Global Transitions Proceedings. 2022; 3(1): 91-99.

(25)Hancock JT, Khoshgoftaar TM. Survey on categorical data for neural networks. J Big Data. 2020; 7: 28.

(26)Guyon I, Elisseeff A. An introduction to variable and feature selection. J Mach Learn Res. 2003; 3: 1157–1182.

(27)Jolliffe IT, Cadima J. Principal component analysis: a review and recent developments. Philos Trans Royal Soc A: Math, Phys Eng Sci. 2016; 374(2065): 20150202.

Reviewer2 3-2

(28)J.M. Bland, D.G. Altman, Comparing methods of measurement: why plotting difference against standard method is misleading, Lancet, 1995; 346(8982): 1085-1087.

(29)Bland JM, Altman DG. Measuring agreement in method comparison studies. Stat Methods Med Res. 1999; 8: 135–60.

(30)Marquardt DW. An Algorithm for Least-Squares Estimation of Nonlinear Parameters. J Soc Indust

Appl Math. 1963; 11(2): 431-41.

(31)Riedmiller M, Braun H. A direct adaptive method for faster backpropagation learning: the RPROP algorithm. In: IEEE Int Conf Neural Netw; 1993; 1: 586-91.

(32)Hoerl AE, Kennard RW. Ridge regression: biased estimation for nonorthogonal problems. Technometrics. 1970; 12(1): 55-67.

Reviewer1 2-2

Supplemental material

S1. Generalized Linear Model (GLM)

For standardized predictors $X \in \mathbb{R}^{N\times P}$ and target $y \in \mathbb{R}^{N}(\mathrm{Hb_{CPB}})$, we fit a Gaussian-identity GLM:

$$y = \beta_0 + X\beta + \varepsilon, \quad \varepsilon \sim \mathcal{N}(0, \sigma^2 I). \tag{s-i}$$

Parameters (β_0, β) were estimated by maximum likelihood (equivalently, least squares under (i)).

Implementation used MATLAB fitglm (MathWorks) with default options.

S2. Support Vector Regression (SVR)

We used ε-SVR with radial basis function (RBF) kernel as shown in the following equation:

$$K(x_i, x_j) = \exp(-\frac{\| x_i - x_j\|^2}{2\sigma^2}). \tag{s-ii}$$

A ε-SVR model is obtained by solving the convex optimization problem as follows:

$$\min_{w,b,\xi,\xi^*} \frac{1}{2}\|w\|^2 + C\sum_{i=1}^{n} \xi_i + \xi_i^*, \tag{s-iii}$$

$$\text{subject to } \begin{cases} y_i - (w^T\phi(x_i) + b) \le \varepsilon + \xi_i, \\ (w^T\phi(x_i) + b) - y_i \le \varepsilon + \xi_i^*, \\ \xi_i, \xi_i^* \ge 0, \ i = 1, \dots, n, \end{cases}$$

where ϕ is the mapping to the feature space, C is the penalty constant (BoxConstraint), and ε is the width of the epsilon-insensitive zone. The predicted Hb concentration $\hat{y}(x)$ is then expressed as a linear combination of support vectors, as follows:

$$\hat{y}(x) = \sum_{i\in S} \alpha_i K(x_i, x) + b, \qquad S = \{i | \alpha_i \neq 0\}. \tag{s-iv}$$

We tuned $(C, \sigma, \gamma, \varepsilon)$ by cross-validation. Implementation used MATLAB fitrsvm with RBF kernel;

expected-improvement-plus criterion in 10-fold CV guided selection.

S3. Multilayer Perceptron (MLP)

We used a feed-forward network with $L-1$ hidden layers. For an input $x \in \mathbb{R}^P$, the layer outputs were defined as:

$$\mathbf{h}^{(l)} = \phi\left(\mathbf{W}^{(l)}\mathbf{h}^{(l-1)} + \mathbf{b}^{(l)}\right), \qquad \mathbf{h}^{(0)} = \mathbf{X}. \tag{s-v}$$

with the final prediction given by:

$$\hat{\boldsymbol{y}} = \mathbf{W}^{(L)}\mathbf{h}^{(L-1)} + \mathbf{b}^{(L)}, \tag{s-vi}$$

The weights $\{W^{(\ell)}, b^{(\ell)}\}$were learned by backpropagation using either the Levenberg–Marquardt or Resilient Backpropagation algorithm (31, 32), with learning rates 10^{-3}or $10^{-4}$and early-stopping patience of 10 or 20 epochs. Model selection followed a nested cross-validation scheme with 5 outer folds and a 5-fold inner grid search over hidden-layer sizes [4], [8], [16], [32], [32, 16], [64, 32], [128, 64], algorithm $\in$ {LM,RProp}, learning rate $\in \{10^{-3}, 10^{-4}\}$, and early-stopping tolerance $\in$ {10,20}. On the full standardized predictor matrix X, the selected configuration was [4] (one hidden layer with 4 neurons) trained with LM at a learning rate of 10^{-3}, early stopping of 10 epochs, and L2 weight decay of 0.1 (33); five random initializations were run and the model with the lowest validation MSE was retained.

S4. Dimensionality Reduction via PCA.

Continuous variables were z-score standardized and categorical variables were one-hot encoded. Principal component analysis (PCA) was then applied to the full predictor matrix to obtain the score matrix $P \in \mathbb{R}^{N \times P_{\mathrm{PCA}}}$. The retention rule was prespecified as "keep the smallest number of components whose cumulative explained variance reaches at least 90%." Component loadings were computed to support interpretability.

S5. Cross-validation, Metrics, and Comparative Baselines.

For model validation, SVR/MLP used standard train–validation splits with reporting on the final fit; SVR employed 10-fold cross-validation for hyperparameter selection and cross-validated error estimates; and MLP used nested 5×5 cross-validation for model selection with outer-fold performance reported. Model performance was summarized uniformly using R^2 and MSE, and agreement between predicted and measured values was assessed with Bland–Altman analysis (bias and 95% limits of agreement). Two published TBV-based formulas were included as comparative baselines; all models (baselines and proposed) were evaluated under the same preprocessing and validation procedures.

Table 1

Index	Total (n=577)	Male (n=447)	Female (n=130)
Demographics			
Age of surgery (years)	66.9 ± 11.6	66.1 ± 11.8	69.5 ± 10.6
Height (cm)	163.0 ± 9.2	167.0 ± 7.31	153.0 ± 6.42
Weight (kg)	63.6 ± 12.3	66.2 ± 11.5	54.8 ± 10.5
Body mass index (kg/m^2)	23.8 ± 3.8	23.8 ± 3.66	23.5 ± 4.16
Body surface area (m^2)	1.68 ± 0.18	1.74 ± 0.16	1.50 ± 0.14
Activated clotting time (s)	117.0 ± 17.3	118.0 ± 17.0	114.0 ± 18.0
LV fraction			
Good	202 (35.0%)	140 (31.3%)	62 (47.7%)
Med	336 (58.2%)	275 (61.5%)	61 (46.9%)
Bad	39 (6.8%)	32 (7.2%)	7 (5.4%)
Laboratory Data			
Creatinine (mg/dL)	0.97 [0.47]	1.01 [0.44]	0.76 [0.39]
Glucose (mg/dL)	109 [26]	109 [26]	110 [23]
Potassium (mEq/L)	3.9 [0.5]	3.9 [0.6]	3.8 [0.6]
Lactic acid (mg/dL)	5.5 [3.4]	5.6 [3.3]	5.0 [3.6]
Hb (g/dL, before CPB)	12.6 [1.8]	12.7 [1.85]	11.9 [1.6]
Hb (g/dL, initiation of CPB)	8.3 [1.4]	8.5 [1.4]	7.8[1.1]
pH	7.39 [0.07]	7.39 [0.07]	7.40 [0.07]
Po_2 (mmHg)	450 [219]	456 [214]	419 [263]
Pco_2 (mmHg)	44.2 [9.30]	44.9 [9.40]	42.3 [8.15]
HCO_3^-(mEq/L)	26.8 [3.30]	26.8 [3.30]	26.8 [3.75]
Blood Volume Estimations			
Ideal weight (kg)	58.9 ± 6.6	61.1 ± 5.4	51.3 ± 4.3
TBV (mL)	5088 ± 981	5293 ± 923	4384 ± 839
Priming Volumes			
Static circuit vol. (mL)	1406 ± 125	1412 ± 128	1386 ± 112
Medical History	Yes	No	Unknown
CHF	32 (5.6%)	535 (92.7%)	10 (1.7%)
CLD	6 (1.0%)	560 (97.1%)	11 (1.9%)
Smoking	230 (39.9%)	332 (57.5%)	15 (2.6%)
Diabetes	170 (29.5%)	396 (68.6%)	11 (1.9%)
Arrhythmia	37 (6.4%)	530 (91.9%)	10 (1.7%)
Hypertension	389 (67.4%)	181 (31.4%)	7 (1.2%)
Hyperlipidemia	260 (45.1%)	307 (53.2%)	10 (1.7%)
Non-cardiac VD	11 (1.9%)	553 (95.8%)	13 (2.3%)
Cerebral VD	16 (2.8%)	549 (95.1%)	12 (2.1%)
Renal failure	107 (18.6%)	463 (80.2%)	7 (1.2%)
Dialysis	52 (9.0%)	518 (89.8%)	7 (1.2%)

The data, except for laboratory data, are presented as mean ± S.D. or number (%). Laboratory data are presented as medians [IQR]. LV: left ventricular; CHF: chronic heart failure; CLD: chronic lung disease; VD: vascular disease; Hb: hemoglobin; TBV: total blood volume; CPB: cardiopulmonary bypass.

Table 2

Component	Estimate	p-value
Intercept	8.48	$< 1 \times 10^{-308}$
PC1	0.173	3.56×10^{-29}
PC2	−0.0665	2.15×10^{-3}
PC3	0.0207	3.70×10^{-1}
PC4	−0.0329	1.76×10^{-1}
PC5	0.245	4.79×10^{-17}
PC6	0.0588	6.19×10^{-2}
PC7	-0.0612	6.16×10^{-2}
PC8	−0.1579	7.66×10^{-6}
PC9	−0.0149	6.76×10^{-1}
PC10	−0.0466	2.11×10^{-1}
PC11	−0.0510	1.86×10^{-1}
PC12	0.251	4.86×10^{-10}
PC13	-0.0396	3.29×10^{-1}
PC14	-0.2184	8.88×10^{-7}
PC15	0.0533	2.55×10^{-1}
PC16	0.0738	1.57×10^{-1}
PC17	0.0822	1.63×10^{-1}

Table 3

Model	MSE	R^2 (adjusted R^2)
GLM	0.797	0.429 (0.369)
PCR	0.808	0.371 (0.352)
SVR	0.517	0.489
SVR with PCA	0.520	0.390
MLP	0.669 ± 0.086	0.332 ± 0.033
MLP with PCA	0.646 ± 0.068	0.352 ± 0.054

MSE: mean squared error; R^2: coefficient of determination; GLM: general linear model; PCR: principal component regression; SVR: support vector regression; PCR: principal component analysis; MLP: multilayer perceptron

Legends

List of Tables

Figure

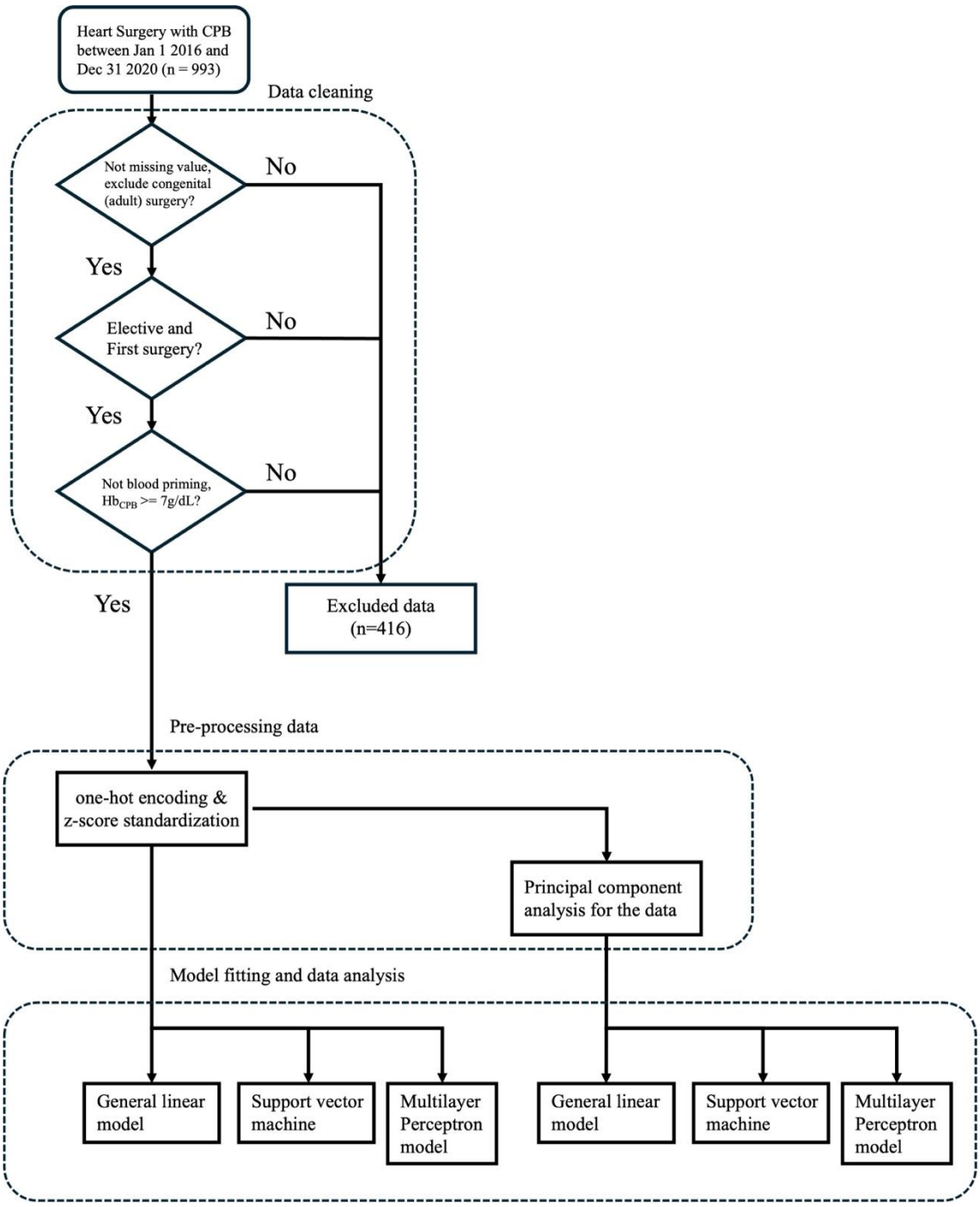

Figure 1

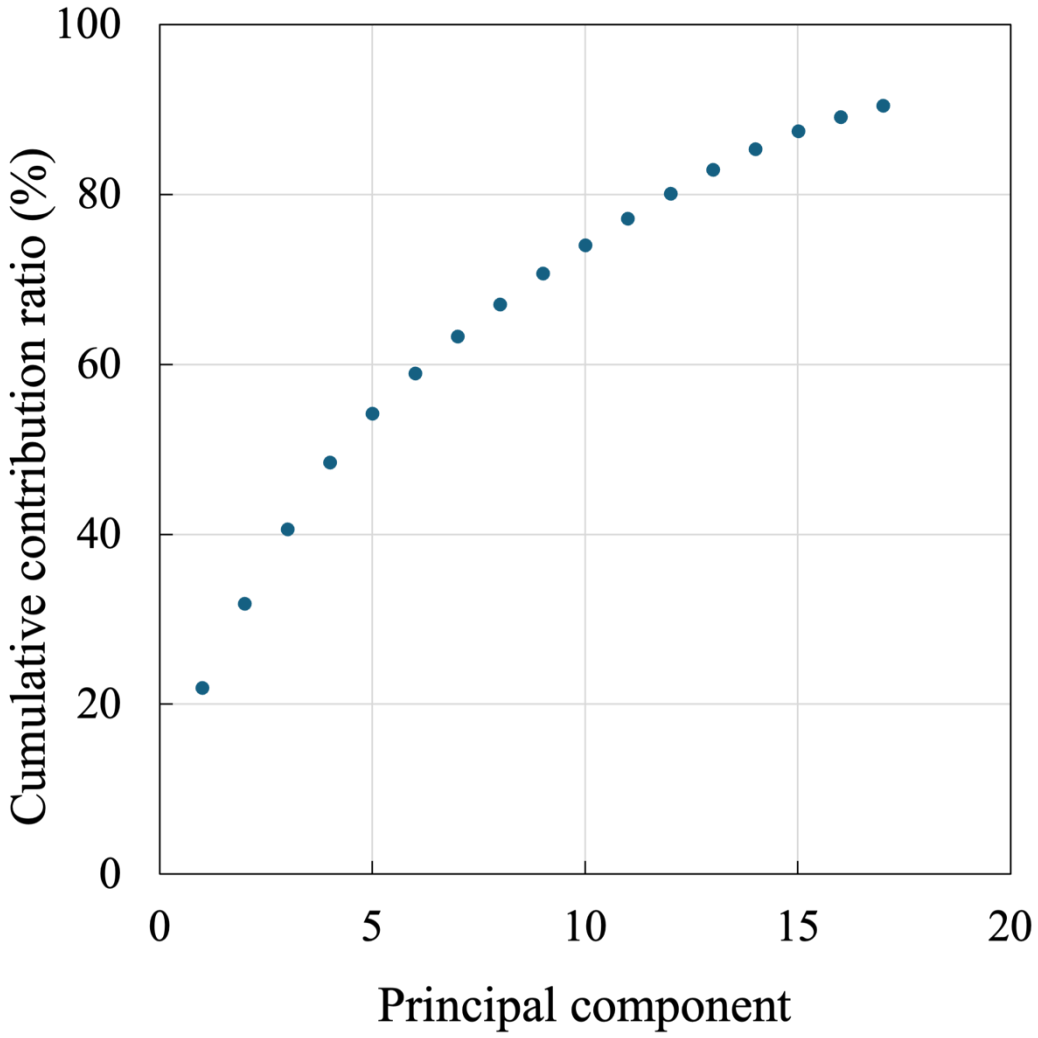
100
80
60
40
20
0
Cumulative contribution ratio (%)
0
5
10
15
20
Principal component

Figure 2

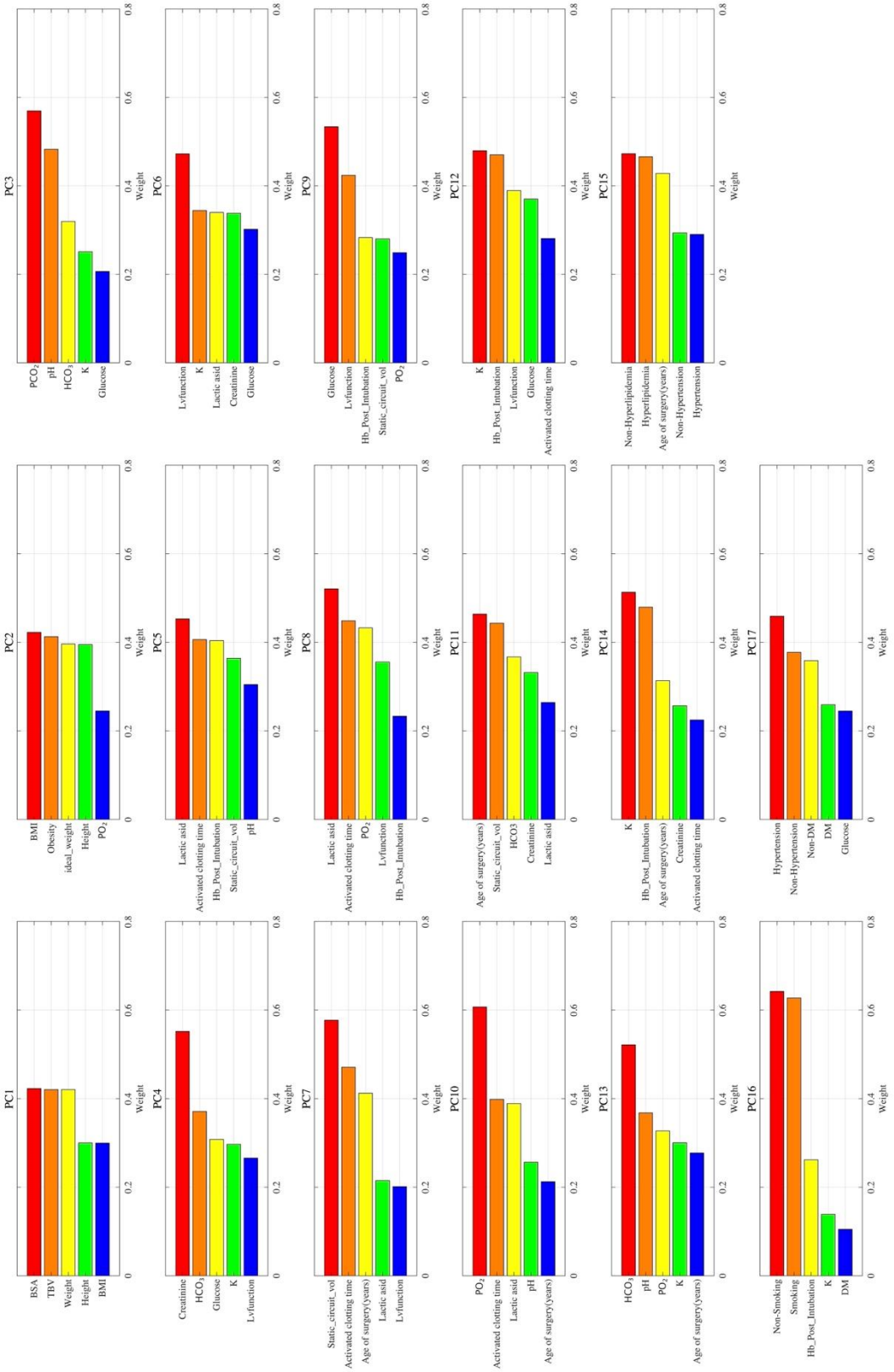
PC1
BSA
TBV
Weight
Height
BMI
PC2
BMI
Obesity
ideal_weight
Height
PO2
PC3
PCO2
pH
HCO3
K
Glucose
PC4
Creatinine
HCO3
Glucose
K
Lvfunction
PC5
Lactic asid
Activated clotting time
Hb_Post_Intubation
Static_circuit_vol
pH
PC6
Lvfunction
K
Lactic asid
Creatinine
Glucose
PC7
Static_circuit_vol
Activated clotting time
Age of surgery(years)
Lactic asid
Lvfunction
PC8
Lactic asid
Activated clotting time
PO2
Lvfunction
Hb_Post_Intubation
PC9
Glucose
Lvfunction
Hb_Post_Intubation
Static_circuit_vol
PO2
PC10
PO2
Activated clotting time
Lactic asid
pH
Age of surgery(years)
PC11
Age of surgery(years)
Static_circuit_vol
HCO3
Creatinine
Lactic asid
PC12
K
Hb_Post_Intubation
Lvfunction
Glucose
Activated clotting time
PC13
HCO3
pH
PO2
K
Age of surgery(years)
PC14
K
Hb_Post_Intubation
Age of surgery(years)
Creatinine
Activated clotting time
PC15
Non-Hyperlipidemia
Hyperlipidemia
Age of surgery(years)
Non-Hypertension
Hypertension
PC16
Non-Smoking
Smoking
Hb_Post_Intubation
K
DM
PC17
Hypertension
Non-Hypertension
Non-DM
DM
Glucose
Weight
0
0.2
0.4
0.6
0.8

Figure 3

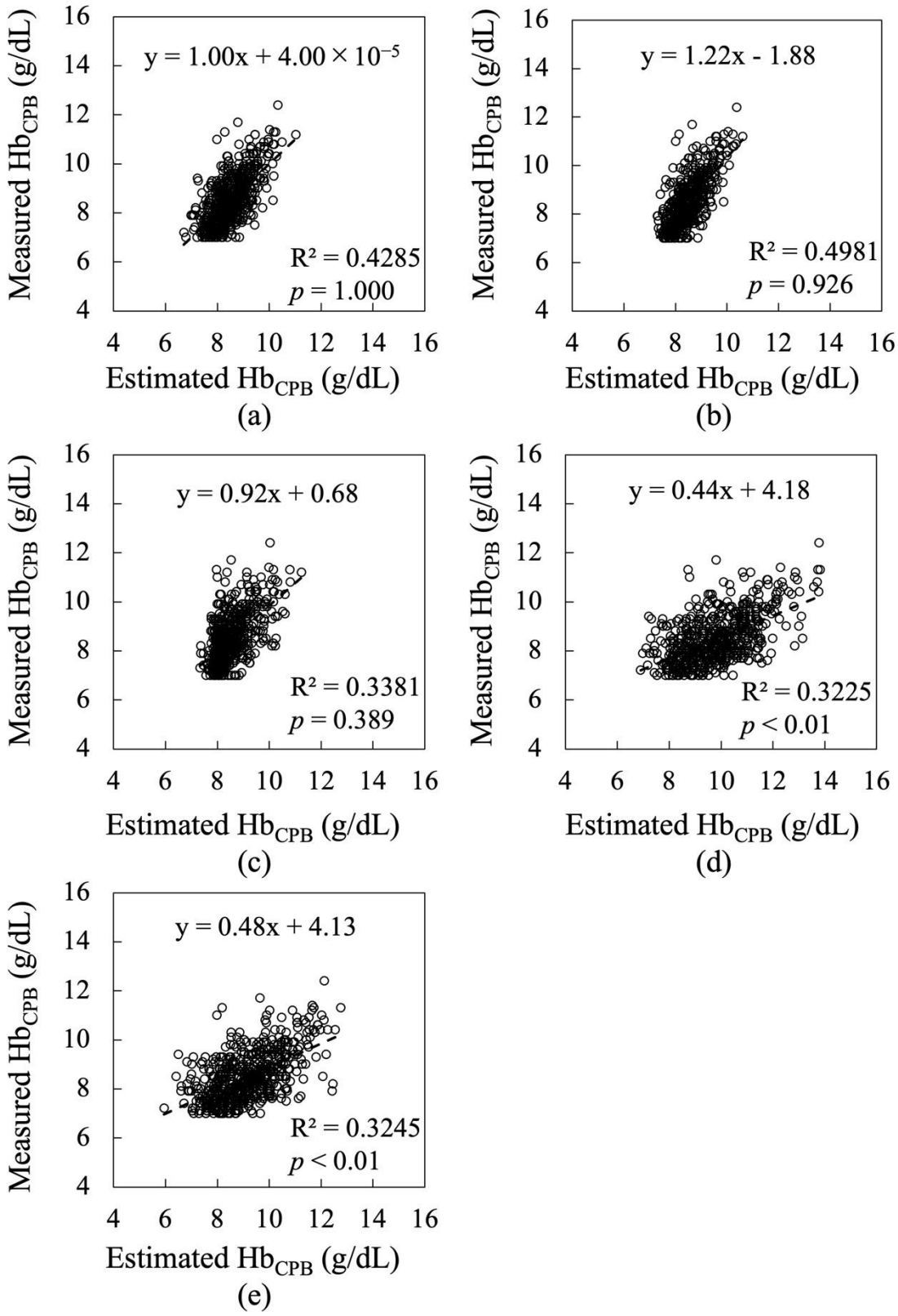
y = 1.00x + 4.00 × 10−5
R² = 0.4285
p = 1.000
Measured HbCPB (g/dL)
Estimated HbCPB (g/dL)
(a)
y = 1.22x - 1.88
R² = 0.4981
p = 0.926
Measured HbCPB (g/dL)
Estimated HbCPB (g/dL)
(b)
y = 0.92x + 0.68
R² = 0.3381
p = 0.389
Measured HbCPB (g/dL)
Estimated HbCPB (g/dL)
(c)
y = 0.44x + 4.18
R² = 0.3225
p < 0.01
Measured HbCPB (g/dL)
Estimated HbCPB (g/dL)
(d)
y = 0.48x + 4.13
R² = 0.3245
p < 0.01
Measured HbCPB (g/dL)
Estimated HbCPB (g/dL)
(e)

Figure4

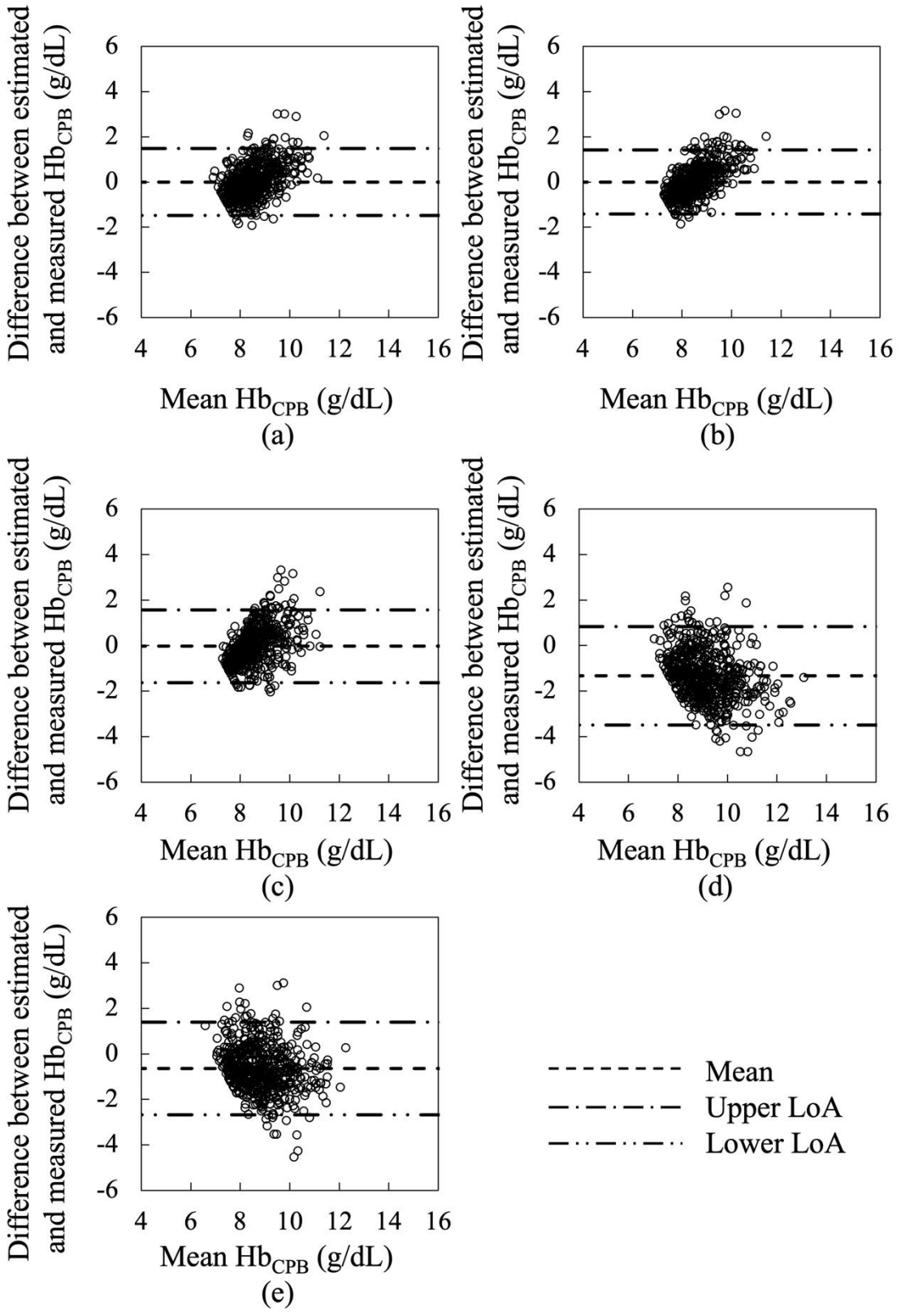
Difference between estimated and measured Hb$_{CPB}$ (g/dL)
6
4
2
0
-2
-4
-6
4
6
8
10
12
14
16
Mean Hb$_{CPB}$ (g/dL)
(a)
(b)
(c)
(d)
(e)
Mean
Upper LoA
Lower LoA

Figure5

Legends

List of Figures

Figure 1: Analysis flowchart

Figure 2: Cumulative explained variance. Principal components (PCs) are added sequentially from PC1 to PC17 (left to right); 90% cumulative explained variance is achieved with the first 17 PCs

Figure 3: Weight of principal component analysis

Figure 4: Correlation between measured Hb_{CPB} and estimated Hb_{CPB}: (a) Hb_{CPB} was estimated based on GLM, (b) that based on SVR, (c) that based on MLP, (d) that calculated based on reference (11), and (e) that based on Equation (11).

Figure 5: Bland–Altman analysis between measured Hb_{CPB} and estimated Hb_{CPB}: (a) estimated Hb_{CPB} was estimated based on GLM, (b) that based on SVR, (c) that based on MLP, (d) that calculated based on reference (11), and (e) that based on equation (11).

The Journal of EXTRACORPOREAL Technology

Raymond Wong, PhD CCP
Editor
Journal of ExtraCorporeal Technology
rkwong@email.arizona.edu

CONFLICT OF INTEREST

JECT requires authors to disclose any commercial association that might pose a conflict of interest with the submitted manuscript by completing the Conflict of Interest statement listed below. It is the responsibility of the authors to fully disclose institutional or corporate affiliations that might constitute a conflict. Any association that results in financial exchange between the author(s) and a private corporation, or entity, must be disclosed. These include consultancies, stock ownership, patent-licensing or similar relationships. If commercial products are evaluated (not just listed in the methodology), the authors are required to include in their cover letter the following:

Conflict of Interest Statement: (please check only one box and sign below)

I declare on behalf of myself and all authors the following:

☑ We **do not** have any material, financial, or other relationship with any healthcare-related business or other entity whose products or services may be discussed in, or directly affected in the marketplace by, this manuscript.

☐ The below-listed authors **do have** a material, financial, or other relationship with a healthcare-related business or other entity whose products or services may be discussed in, or directly affected in the marketplace by, this manuscript. This relationship is specified below.

Signature of Senior Author 日比谷 誠 (HIBIYA Makoto)

All funding sources supporting the work will be acknowledged at the end of the manuscript. If the editorial staff feels that there is a potential conflict of interest, it must be disclosed in written format. Authors will be apprised of such a decision in writing prior to publication.

Authors name	**Conflict**

/Users/hibiya/Downloads/conflictofinterest.DOC

Estimation of Hemoglobin Concentration at the Initiation of Cardiopulmonary Bypass Using Support Vector Regression

Keywords

hemoglobin, support vector regression, cardiopulmonary bypass, machine learning, hemodilution

Abstract

Background: Hemodilution during cardiopulmonary bypass (CPB) is a standard perfusion strategy used to reduce blood viscosity and enhance microcirculatory flow. The hemodilution rate, expressed as hemoglobin (Hb) concentration, is a key control index in CPB and is currently estimated from total blood volume (TBV). The objective of this study was to propose a novel formula to accurately predict Hb concentration at the initiation of CPB (Hb_{CPB}) by incorporating circulating blood volume, laboratory data, physical measurements, and patient history.

Methods: We retrospectively analyzed 577 adult patients who underwent elective CPB at Fujita Health University Hospital from January 2016 to December 2020. Thirty-six preoperative variables—including demographics, laboratory data, circuit parameters, and indices such as TBV and ideal weight—were standardized. Categorical variables underwent one-hot encoding. We compared generalized linear models (GLM), support vector regression (SVR), and multilayer perceptron (MLP). Model performance was evaluated using the coefficient of determination (R^2), mean squared error (MSE), and Bland–Altman analysis (bias and 95% limits of agreement [LoA]). Predictions from two

conventional TBV-based formulas were used as benchmarks.

Results: Of 993 screened cases, 577 met inclusion criteria (447 males, mean age 66.8 ± 11.7 years; 130 females, 69.5 ± 10.6 years). SVR on standardized predictors achieved the highest accuracy (R^2 = 0.498, MSE = 0.517), outperforming GLM (R^2 = 0.429, MSE = 0.797) and MLP (R^2 = 0.332, MSE = 0.669). Conventional formulas showed lower performance (R^2 = 0.325, MSE ≥ 1.48). Bland–Altman analysis for SVR demonstrated minimal bias (–0.0028 g/dL) and narrower LoA (–1.42 to 1.41 g/dL) than conventional methods (bias –1.33 g/dL; LoA –3.49 to 0.83 g/dL).

Conclusion: These findings suggest that an SVR-based model improves prediction of Hb_{CPB} over conventional approaches, supporting optimized transfusion management and reduced hemodilution-related risks.

Introduction

Japan's population is aging rapidly, and the proportion of elderly patients undergoing cardiac surgery with cardiopulmonary bypass (CPB) has steadily increased over the past decade (1–4). As this trend is expected to continue, developing appropriate CPB technologies for older patients has become imperative. Hemodilution during CPB is a standard perfusion strategy used to reduce blood viscosity and enhance microcirculatory flow (5). However, anemia resulting from hemodilution may cause ischemic organ injury, increase mortality, and elevate stroke risk (6, 7, 8). Current guidelines recommend maintaining hematocrit (Ht) levels ≥ 21% and/or hemoglobin (Hb) concentrations ≥ 7.0 g/dL during CPB to minimize hemodilution-related complications (9, 10, 11). To assess the hemodilution rate, total blood volume (TBV) is estimated using body weight in kilograms (kg). TBV estimates are typically set at 70 mL/kg for American adult males, 65 mL/kg for females (12, 13), and 80 mL/kg for Japanese adults (14). This method is commonly applied to all adults, regardless of age. However, several studies have shown discrepancies between predicted post-dilution Ht or Hb values and actual Hb concentrations at the initiation of CPB (Hb_{CPB}) (15–17). Revised formulas incorporating sex and age have been proposed to improve TBV estimates (18). Nonetheless, these methods often lack applicability to older patients, as they do not adequately account for age-related TBV decline (19).

This study aims to develop and propose a novel formula to predict Hb_{CPB} more accurately by

incorporating TBV, laboratory data, physical measurements, and clinical history.

Materials and Methods

Clinical data

This study analyzed data that were prepared to register in the Perfusion Database maintained by the Japanese Society of Extra-Corporeal Technology in Medicine (JaSECT) for patients who underwent cardiac surgery with CPB at Fujita Health University Hospital between January 1, 2016, and December 31, 2020. Only elective cases were included. Patients with congenital heart disease or those who underwent repeat surgeries were excluded to avoid duplicate entries, particularly in preoperative background data. Additionally, cases involving blood priming or with hemoglobin (Hb) concentrations below 7 g/dL at CPB initiation were excluded. Details of the data cleaning process are shown in Figure 1. The JaSECT Perfusion Database collects data across six domains: patient demographics; circuit and priming fluid details; CPB parameters; fluid volume input and output management; laboratory data and outcomes. These domains consist of 84 multiple-choice items and 159 numeric variables, totaling 243 parameters (20). From in-hospital data for this database, we extracted 35 pre-CPB parameters along with $\mathrm{Hb}_{\mathrm{CPB}}$ for model development, as described in the following section.

- **Demographic and clinical variables**: sex; age at surgery; surgical procedure; height; weight;

left ventricular ejection fraction; and risk factors, including congestive heart failure, chronic respiratory disease, smoking history, diabetes mellitus, arrhythmia, hypertension, dyslipidemia, cardiovascular or extracardiac vascular disease, cerebrovascular disease, renal dysfunction, and chronic dialysis.

- **Blood laboratory data obtained by the time of admission to the operating room**: glucose (mg/dL); potassium (mEq/L); lactate (mg/dL); creatinine (mg/dL); Hb (g/dL); results of arterial blood gas analysis (pH, PaO_2(mmHg), $PaCO_2$(mmHg), HCO_3^-(mEq/L)) and activated clotting time (sec)
- **Variables described the CPB circuit configuration**: biocompatible coating part; planned priming volume (Static circuit volume); and priming fluid composition.
- **Variables obtained from formulas using collected data**: ideal body weight; TBV; body mass index (BMI); obesity classification; and body surface area (BSA).

BMI, ideal body weight (BW_i) (18), TBV (11) and BSA (21) were calculated as follows (Equations (i)–(iv)):

$$\text{BMI} = \frac{w}{h^2}, \quad \text{(i)}$$

$$\text{BW}_\text{i} = 22h^2, \quad \text{(ii)}$$

$$\text{TBV} = 80w, \quad \text{(iii)}$$

$$\text{BSA} = 0.7184 \times 10^{-4} \times h^{0.725} \times w^{0.425}, \quad \text{(iv)}$$

where w is the body weight (kg) and h is the height (m).

Obesity was classified according to the Japanese Society for the Study of Obesity Guidelines (22) as follows: underweight (BMI < 18.5 kg/m^2), normal weight (18.5 ≤ BMI < 25 kg/m^2), obesity class I (25 ≤ BMI < 30 kg/m^2), class II (30 ≤ BMI < 35 kg/m^2), class III (35 ≤ BMI < 40 kg/m^2), and class IV (BMI ≥ 40 kg/m^2). Hematocrit (Ht) values measured before and at CPB initiation were converted to Hb concentrations using the equation: $\mathrm{Ht} \approx 3 \times \mathrm{Hb}$ (23).

Analysis protocol

Preprocessing of eligible Clinical Data

The 35 parameters described in the previous section were considered candidate explanatory variables for estimating $\mathrm{Hb}_{\mathrm{CPB}}$. One-hot encoding was applied to 15 categorical variables (e.g., sex, type of surgery, and presence of comorbidities), and z-score standardization was applied to 20 continuous variables (e.g., laboratory data) (24, 25). The interactions among variables, and between each variable and hemoglobin concentration, remain unknown. In general, including variables with low or no relevance to the target variable may impair the generalizability of a predictive model and lead to overfitting. It is therefore advisable to limit explanatory variables to those that carry significant information about the outcome (26). However, this restriction may exclude potentially informative features. To address this, we prepared two datasets for analysis: the full standardized dataset and a

dimensionally reduced dataset, described below.

Principal Component Analysis (PCA) (27) was applied to the standardized explanatory matrix $\mathbf{X} \in \mathbb{R}^{N\times P}$ (where N is the number of subjects and P is the number of variables) to mitigate multicollinearity. Eigenvalue decomposition was performed on the covariance matrix $\Sigma = \frac{1}{N-1}, \mathbf{X}^{\mathrm{T}}\mathbf{X}$, and the smallest number of principal components K was selected such that the cumulative contribution of the eigenvalues $\lambda_k{}_{k=1}^{P}$ exceeded 90 %. Next, the principal component score matrix $\mathbf{P} = [\mathbf{t}_1, \dots, \mathbf{t}_K,] = \mathbf{X}[\mathbf{v}_1, \dots, \mathbf{v}_K] \in \mathbb{R}^{N\times K}$ was calculated using the principal component vector $v_k{}_{k=1}^{K}$. After PCA, $\mathbf{P}$ was used as the explanatory variable for the subsequent model training.

Linear model for predicting hemoglobin concentration at CPB initiation

Conventional methods for estimating $\mathrm{Hb}_{\mathrm{CPB}}$ (17–19) are essentially linear models that incorporate a limited set of patient and circuit factors, such as priming volume. We first evaluated whether a linear approach would be adequate for our dataset. To do so, we fit a generalized linear model (GLM) using routinely available pre-CPB variables, including body size indices, laboratory values, and circuit settings. The GLM assumes that $\mathrm{Hb}_{\mathrm{CPB}}$ varies in approximate proportion to changes in these inputs. Model performance was assessed using the coefficient of determination (R^2) and mean squared error (MSE). The explicit GLM equation and estimation procedures are provided in Supplementary Equation (S-i).

Nonlinear model for predicting hemoglobin concentration at CPB initiation

Because clinical data often contain nonlinear relationships and interactions that linear models may not capture, we also evaluated two standard nonlinear approaches: Support Vector Regression (SVR) and a Multilayer Perceptron (MLP).

SVR can model curved relationships between the inputs and Hb_{CPB} without the need to specify functional forms. We used a widely adopted SVR implementation and tuned its hyperparameters by cross-validation to reduce overfitting; further details are provided in the Supplement (equations s-ii, iii). The MLP is a simple neural-network model that learns patterns by stacking a small number of layers. We compared several compact architectures and training configurations and selected the model that performed best in cross-validation. Training details (architecture and stopping criteria) are summarized in the Supplement (equation s-iv).

For some analyses, we also used a compressed set of input variables derived from principal component analysis to reduce redundancy among predictors. We retained the smallest number of components that preserved approximately 90% of the total variance. Technical details are provided in Supplement S2.

Model training, validation, and reporting

For all models, we standardized inputs when appropriate, tuned model settings by cross-validation, and summarized performance using $R^2$and MSE. Because correlation-based indices do not measure exact agreement, we also evaluated agreement between predicted and measured $\mathrm{Hb}_{\mathrm{CPB}}$ with Bland–Altman analysis (bias and 95% limits of agreement).

Software and reproducibility

Analyses were performed with commonly used, off-the-shelf software (e.g., MATLAB equivalents or open-source alternatives). Parameter settings and code snippets sufficient for reproduction are listed in the Supplement.

Evaluation of the proposed method

To evaluate the performance of the trained models, predictions on the validation and hold-out test sets were computed and compared against the reference values of $\mathrm{Hb}_{\mathrm{CPB}}$. As this is a regression task, three metrics were used to quantify prediction accuracy: MSE, mean absolute error, and the coefficient of determination (R^2). In addition, Bland–Altman analysis was performed to further examine the agreement between predicted and measured hemoglobin concentrations. From this analysis, the mean difference (bias) and 95% limits of agreement (LoA), defined as ±1.96 times the standard deviation of

the differences, were calculated.

To benchmark our method against conventional prediction models, the same clinical dataset was fitted using the standard hematocrit-based prediction formula (18), which is expressed as:

$$\mathrm{Ht_{CPB}} = \mathrm{Ht_{beforeCPB}} \times (1 - \frac{\mathrm{PV}}{\mathrm{PV} + \mathrm{TBV}}), \quad \text{(v)}$$

where $\mathrm{Ht_{CPB}}$ is the hematocrit value under CPB, $\mathrm{Ht_{beforeCPB}}$ is the hematocrit value before CPB, PV is Priming Volume. TBV was substituted from two approaches: Equation (iii) (19) and the following equation (18):

$$\mathrm{TBV} = \begin{cases} 70 \times \mathrm{BW} & (\mathrm{Age} < 65) \\ 60 \times BW & (\mathrm{Age} \geq 65) \end{cases}, \quad \text{(vi)}$$

Estimated Hb concentrations based on Equation (v) and their Bland–Altman statistics, mean difference, and 95 % LoA, were compared with those obtained for our approach.

Results

Data from 577 patients, including 447 males (mean age 66.1 ± 11.8 years) and 130 females (mean age 69.5 ± 10.6 years), were included in the analysis. Subject characteristics are summarized in Table 1. In terms of obesity classification, 31 patients (5.4%) were underweight, 361 (62.6%) were standard weight, 146 (25.3%) were classified as obese class I, 33 (5.7%) as class II, 5 (0.8%) as class III, and 1 (0.2%) as class IV. The surgical procedures included coronary artery bypass grafting (CABG) in 149 patients (25.8%), valve surgery in 215 (37.3%), combined CABG and valve procedures in 67 (11.6%),

combined CABG and other procedures in 27 (4.7%), aortic surgery in 91 (15.8%), and other procedures in 28 (4.8%). Regarding biopassive coating, it was absent in 2 patients (0.3%), applied to limited components in 34 (5.9%), applied to all components except the cannulae in 484 (84.0%), and applied tip-to-tip in 57 (9.8%). The main priming solution was bicarbonate Ringer's in 540 patients (93.6%). Other solutions included saline in 17 (3.0%), lactated Ringer's in 2 (0.3%), acetate Ringer's in 3 (0.5%), starch or dextran in 3 (0.5%), and other crystalloid-only solutions in 12 (2.1%). A centrifugal pump was employed in all cases.

Figure 2 shows the scree plot of the principal components derived from PCA of the predictor matrix $\mathbf{X} \in \mathbb{R}^{N \times P}$, which comprises z-score standardized continuous variables and one-hot encoded categorical variables. From this plot, it was confirmed that 17 components were required to reach a cumulative explained variance of 90%. Figure 3 illustrates the five variables with the highest absolute loadings for each principal component. These results indicate that body weight was captured primarily by PC1, priming volume (static circuit volume) by PCs 5, 7, 9, and 11, and preoperative hemoglobin concentration by PCs 5, 8, 9, 12, 14, and 16. Table 2 presents the results of the generalized linear model fitted to the PCA-transformed predictors. The analysis revealed that intraoperative $\mathrm{Hb}_{\mathrm{CPB}}$ was primarily determined by six principal components: PC1, PC2, PC5, PC8, PC12, and PC14.

Figure 4 shows the comparison between measured $\mathrm{Hb}_{\mathrm{CPB}}$ and predicted values based on pre-CPB variables, while Table 3 summarizes model performance indices. For each scatter plot in Figure

4, the ordinary least-squares regression slopes and y-intercepts—where better estimation is reflected by a slope close to 1 and a y-intercept close to 0—are displayed. The slopes and intercepts (panels a–e) are as follows: (a) slope = 1.00, intercept = 4.00×10^{-5}; (b) slope = 1.22, intercept = −1.88; (c) slope = 0.92, intercept = 0.68; (d) slope = 0.44, intercept = 4.18; (e) slope = 0.48, intercept = 4.13. A GLM fitted to the standardized predictor matrix $\mathbf{X} \in \mathbb{R}^{N \times P}$ achieved a coefficient of determination of $R^2_{\text{GLM}} = 0.429$, adjusted $R^2_{\text{GLM}} = 0.369$, and $\text{MSE}_{\text{GLM}} = 0.797$. However, multicollinearity in the input matrix was confirmed, resulting in a lack of full rank. Applying the same GLM to PCA-transformed predictors $\mathbf{X}_{\text{PCA}} \in \mathbb{R}^{N \times P_{\text{PCA}}}$ yielded $R^2_{\text{PCR}} = 0.371$ (adjusted $R^2_{\text{PCR}} = 0.352$) and $\text{MSE}_{\text{PCR}} = 0.808$. SVR on $\mathbf{X}$ with optimized hyperparameters $C = 2.279$, $\gamma = 16.81$, and $\varepsilon = 0.594$ yielded $R^2_{\text{SVR}} = 0.498$ and 10-fold CV $\text{MSE}_{\text{SVR}} = 0.517$, outperforming the GLM. When SVR was applied to $\mathbf{X}_{\text{PCA}}$ with $C = 1.662$, $\gamma = 14.28$, and $\varepsilon = 0.0084$, performance decreased to $R^2_{\text{SVR}_{\text{PCA}}} = 0.39$ and CV $\text{MSE}_{\text{SVR}_{\text{PCA}}} = 0.52$. The MLP model, tuned via nested 5-fold CV, selected one hidden-layer architecture of 4 neurons, with Resilient Backpropagation, a learning rate of 10^{-2}, and early stopping tolerance of 10. On $\mathbf{X}$, this configuration yielded $R^2_{\text{MLP}} = 0.332 \pm 0.033$ and $\text{MSE}_{\text{MLP}} = 0.669 \pm 0.086$. When applied to $\mathbf{X}_{\text{PCA}}$, the MLP achieved $R^2 = 0.352 \pm 0.054$ and $\text{MSE} = 0.646 \pm 0.068$. The coefficients of determination from both MLP configurations were lower than those from SVR. Previously published Hb_{CPB} prediction formulas yielded $R^2 = 0.3225$, MSE = 2.98 based on (19), and $R^2 = 0.3245$, MSE = 1.48 based on (18), both substantially lower

than SVR performance.

Figure 5 displays the Bland–Altman analysis results. The bias between predicted and measured GLM values was -5×10^{-7} g/dL (95% CI: -0.0654 to 0.0654 g/dL), with 95% LoA of [–1.57 g/dL, 1.57 g/dL]. For SVR, the bias was –0.0028g/dL (95% CI: -0.0619 to 0.0562g/dL) with LoA of [–1.41 g/dL, 1.41 g/dL]. For MLP, the bias was –0.029 g/dL (95% CI: -0.0963 to 0.0375g/dL), and LoA was [–1.63 g/dL, 1.57 g/dL]. In contrast, the conventional methods had a bias of –1.33 g/dL (95% CI: –1.41 to –1.24 g/dL) and LoA of [–3.49 g/dL, 0.831 g/dL] for the reference (11) and a bias of –0.64 g/dL (95% CI: –0.72 to –0.555 g/dL) and LoA of [–2.67g/dL, 1.39g/dL] for the Equation (v), respectively. The 95% CI for bias did not include zero, indicating systematic error. In comparison, CIs from GLM, SVR, and MLP included zero, suggesting no statistically significant bias and the absence of systematic error. Biases between measured and predicted $\mathrm{Hb}_{\mathrm{CPB}}$ from GLM, SVR, and MLP were not statistically significant (GLM: $p = 1.000, d = -6.5 \times 10^{-7}$; SVR: $p = 0.926, d = -0.004$; MLP: $p = 0.389, d = -0.036$). Conversely, biases from conventional models were confirmed (reference (11): $p < 0.01, d = -1.21$; Equation (v): $p < 0.01, d = -0.617$).

Discussion

The GLM demonstrated moderate goodness-of-it despite the multicollinearity present in the input parameter matrix $\mathbf{X} \in \mathbb{R}^{N \times P}$. In contrast, implementing PCR resulted in reduced model performance

across all evaluation metrics compared with the GLM. In PCR, dimensionality reduction is driven solely by the variance structure of the predictor matrix; therefore, principal components that explain substantial variance but have limited correlation with the response variable may still be retained as leading components. In this study, the first 17 principal components were adopted, collectively accounting for 90% cumulative explained variance in the predictor matrix. While this approach preserved most of the predictor information, it may have failed to isolate features most relevant to Hb_{CPB}. Furthermore, the first principal component accounted for more than 20% of the total variance, and PC1 and PC2 were primarily composed of weight, height, TBV, BSA, BMI, ideal weight, and obesity measures, supporting the interpretation that TBV-related factors remain central to Hb_{CPB} estimation. As a result, the PCR model may not have adequately captured the most predictive features of Hb_{CPB}, likely contributing to its reduced performance, as reflected in the lower coefficient of determination and higher MSE compared with the GLM using the full predictor set. Traditional predictors used to estimate Hb_{CPB}—including body weight, priming volume (static circuit volume), and preoperative Hb concentration—were embedded within the principal components retained by PCR and were selected as input features for both the SVR and MLP models. Nevertheless, several of the principal components used in Hb_{CPB} prediction did not primarily reflect these conventional parameters. Therefore, Hb_{CPB} cannot be fully explained by body weight, priming volume, and preoperative Hb concentration alone, as suggested by conventional approaches. At the same time,

while models using PCs 1–17 showed better performance than the conventional formula, we cannot presently ascribe the improvement to specific components without dedicated ablation or feature-contribution analyses. These findings highlight the influence of additional confounding variables, including age and comorbidities.

Although model development and training require computational resources (workstation- or cloud-based), inference is lightweight and can be executed on common devices (e.g., a standard laptop or smartphone) with low latency and no specialized hardware. This enables point-of-care use in the operating room as a simple calculator or as a module integrated into existing perfusion workflows. Accordingly, the trained model can be delivered either (i) within the EHR as a point-of-care calculator or clinical decision support widget that auto-populates inputs from routinely collected pre-CPB data, or (ii) on perfusion hardware (e.g., as a vendor plug-in) to present predictions alongside pump parameters. After deployment, the model can operate offline, with input variables populated automatically from routine pre-CPB data, minimizing manual entry and cognitive load.

Among the nonlinear models, SVR demonstrated a higher coefficient of determination and lower MSE compared with both the GLM and PCR, indicating that SVR had superior predictive power. In contrast, applying PCA prior to SVR led to a decreased coefficient of determination, likely due to the exclusion of Hb_{CPB}-related features during the PCA process, as these were among the bottom 10% of

principal components that were subsequently discarded. The MLP model, incorporating Levenberg–Marquardt–based parameter optimization and early stopping, achieved stable training. When applied to the standardized predictor matrix, MLP showed slightly lower performance than SVR but still achieved a moderate goodness-of-fit. Overall, SVR and MLP, which perform nonlinear function estimation and embed variable selection within the model, outperformed linear models, including conventional approaches, in predicting outcomes from high-dimensional medical data.

Although the best-performing method yielded a modest R^2, agreement relevant to bedside use is better captured by Bland–Altman analysis (28, 29): the new methods demonstrated minimal bias and narrower limits of agreement than the conventional formulas (Figure 5), indicating improved agreement despite a moderate R^2 compared with previous methods. Finally, while models using multiple principal components outperformed the conventional formula, we cannot presently ascribe the improvement to specific components without dedicated ablation or feature-contribution analyses; this is noted as a limitation and will be addressed in future work.

Model development and training require computational resources; these activities can be conducted cost-effectively on a workstation or in the cloud using open-source machine-learning frameworks. After training, inference is lightweight, runs on commodity devices without accelerators, and can be embedded in existing EHR or perfusion-system workflows with minimal latency. From a clinical perspective, more accurate prediction of $\mathrm{Hb}_{\mathrm{CPB}}$ at CPB initiation supports optimized

transfusion strategies—reducing the likelihood of both under- and over-transfusion—and may help lower hemodilution-related risks while standardizing practice across teams. We therefore view the cost–benefit balance as favorable, while acknowledging that prospective evaluation of clinical outcomes and a formal cost-effectiveness analysis are warranted in future work.

Limitations

While the proposed models using PCs 1–17 outperformed the conventional formula, we cannot, at present, attribute this improvement to specific principal components without dedicated ablation or feature-contribution analyses. We acknowledge this as a limitation and plan to investigate the contribution of individual components and underlying variables in future work.

Although inference is feasible on standard devices, clinical integration remains ongoing. Both EHR-based and device-based (perfusion console) deployments are feasible, but practical adoption will require: (A) interoperability with hospital systems and/or perfusion consoles, (B) a user interface suited to intraoperative workflow, (C) prospective validation with monitoring for model drift, and (D) security and access control consistent with institutional policies. We plan to evaluate these aspects and conduct prospective usability and safety assessments prior to routine operating-room adoption.

Funding

The authors received no funding to complete this research.

Conflict of Interest

The authors declare no conflict of interest.

Data Availability

Data available upon request from the corresponding author.

Author Contributions

H. H. contributed to the conceptualization and design of the study, performed data analysis, drafted the initial manuscript, and participated in the review and revision of the final version. S. T. conducted statistical analysis, contributed to data interpretation, and assisted in drafting the manuscript. T.K. participated in data analysis and provided a critical review of the manuscript. M. H. contributed to the study's conceptualization and design, provided overall supervision, and critically reviewed and revised the manuscript. All authors read and approved the final manuscript.

Ethics Approval

This study was approved by the Ethics Review Committee of Fujita Health University (Approval No. HM21-381).

Acknowledgement

The authors express their sincere gratitude to Tomoaki Yamashiro, Yusuke Nakamura, and the Clinical Engineering Department staff at Fujita Health University Hospital for their meticulous efforts in data collection.

References

(1) Hirata Y, Hirahara N, Murakami A, Motomura N, Miyata H, Takamoto S. Current status of cardiovascular surgery in Japan: analysis of data from Japan cardiovascular surgery database in 2015, 2016. 1. congenital heart surgery. Jpn J Cardiovasc Surg. 2019; 48(1): 1-5 (in Japanese).

(2) Abe T, Nakano K, Hirahara N, Motomura N, Miyata H, Takamoto S, Current Status of cardiovascular surgery in Japan: analysis of data from Japan cardiovascular surgery database in 2015, 2016. 3-Valvular heart surgery. Jpn J Cardiovasc Surg. 2019; 48(1): 11-7 (in Japanese).

(3) Shimizu H, Hirahara N, Motomura N, Miyata H, Takamoto S. Current status of cardiovascular surgery in Japan: analysis of data from Japan cardiovascular surgery database in 2015, 2016. 4-Thoracic aortic surgery. Jpn J Cardiovasc Surg. 2019; 48(1): 18-24 (in Japanese).

(4) Saito A, Hirahara N, Motomura N, Miyata H, Takamoto S. Current status of cardiovascular surgery in Japan: analysis of data from Japan cardiovascular surgery database in 2015, 2016. 2. Isolated Coronary Artery Bypass Surgery. 2-Isolated coronary artery bypass surgery. Jpn J Cardiovasc Surg. 2019; 48(1): 6-10 (in Japanese).

(5) Taniguchi FP, Martins AS. Hemodilution, kidney dysfunction and cardiac surgery. Einstein (Sao Paulo). 2009;7(1 Pt 1):103-7.

(6) Ranucci M, Conti D, Castelvecchio S, et al. Hematocrit on cardiopulmonary bypass and outcome after coronary surgery in nontransfused patients. Ann Thorac Surg. 2010; 89(1): 11-17.

(7) Karkouti K, Djaiani G, Borger MA, et al. Low hematocrit during cardiopulmonary bypass is associated with increased risk of perioperative stroke in cardiac surgery. Ann Thorac Surg. 2005; 80(4): 1381-1387.

(8) Tsui AKY, Dattani ND, Marsden PA, et al. Reassessing the risk of hemodilutional anemia: Some new pieces to an old puzzle. Can J Anaesth. 2010; 57(8): 779-791.

(9) Boer C, Meesters MI, Milojevic M et al. 2017 EACTS/EACTA Guidelines on patient blood management for adult cardiac surgery. J Cardiothorac Vasc Anesth. 2018; 32(1): 88-120.

(10) Ferraris VA, Brown JR, Despotis GJ et al. 2011 Update to The Society of Thoracic Surgeons and the Society of Cardiovascular Anesthesiologists Blood Conservation Clinical Practice Guidelines**The International Consortium for Evidence Based Perfusion formally endorses these guidelines. Ann Thorac Surg. 2011; 91(3): 944-982.

(11) Murphy GS, Hessel EA, Groom RC et al. Optimal perfusion during cardiopulmonary bypass: an evidence-based approach. Anesth Analg. 2009; 108(5): 1394-1417.

(12) Gravlee GP. Cardiopulmonary bypass: principles and practice. 3rd ed. Philadelphia, PA: Lippincott Williams & Wilkins; 2008: 416-417.

(13) Hall JE. Guyton and Hall Textbook of Medical Physiology. 14th ed. Philadelphia, PA: Elsevier; 2020: 305-310.

(14) Sonoki T, Mushino T, Ueda Y et al., Use guidelines on red blood cell preparation based

on scientific grounds (the revision third edition). Jpn J Transfusion Cell Therapy. 2024; 70(6): 579—596 (in Japanese).

(15)Hilberath J, Thomas ME, Smith T et al. Blood volume measurement by hemodilution: association with valve disease and re-evaluation of the Allen Formula. Perfusion. 2015; 30(4): 305-311.

(16)Hasegawa T, Iba Y, Naraoka S et al. Improvement of predicted hematocrit values after the initiation of cardiopulmonary bypass in cardiovascular surgery. J Artif Organs. 2021; 25: 1-8.

(17)Trowbridge C, Stammers A, Klayman M, Brindisi N. A Novel Calculation to Estimate Blood Volume and Hematocrit During Bypass. J Extra Corpor Technol. 2008; 40(1): 61-4.

(18)Muraki R, Hiraoka A, Nagata K et al. Novel method for estimating the total blood volume: the importance of adjustment using the ideal body weight and age for the accurate prediction of haemodilution during cardiopulmonary bypass. Interact Cardiovasc Thorac Surg. 2018; 27(6): 802-7.

(19)Erpicum M, Dardenne N, Hans G, Larbuisson R, Defraigne JO. Prediction of the post-dilution hematocrit during cardiopulmonary bypass. Are new formulas needed? Perfusion. 2016; 31(6): 458-464.

(20)Hibiya M, Kamei T, Kubota S et al. Study profile of the perfusion registry in Japan. Jpn J Extra Corpor Technol. 2018; 45(1): 1-7.

(21)Du Bois D, Du Bois EF. A formula to estimate the approximate surface area if height and weight

be known. Arch Int Med. 1916; 17(6): 863-871.

(22) Japan Society for the Study of Obesity. Guidelines for the management of obesity disease 2022. Tokyo: Life Science Publishing; 2022: 1-7 (in Japanese).

(23) Shin DA, Lee JC, Shin H, Cho YJ, Kim HC. Point-of-care testing of plasma free hemoglobin and hematocrit for mechanical circulatory support. Sci Rep. 2021; 11(1): 3788.

(24) Maharana K, Mondal S, Nemade B. A review: Data pre-processing and data augmentation techniques. Global Transitions Proceedings. 2022; 3(1): 91-99.

(25) Hancock JT, Khoshgoftaar TM. Survey on categorical data for neural networks. J Big Data. 2020; 7: 28.

(26) Guyon I, Elisseeff A. An introduction to variable and feature selection. J Mach Learn Res. 2003; 3: 1157–1182.

(27) Jolliffe IT, Cadima J. Principal component analysis: a review and recent developments. Philos Trans Royal Soc A: Math, Phys Eng Sci. 2016; 374(2065): 20150202.

(28) J.M. Bland, D.G. Altman, Comparing methods of measurement: why plotting difference against standard method is misleading, Lancet, 1995; 346(8982): 1085-1087.

(29) Bland JM, Altman DG. Measuring agreement in method comparison studies. Stat Methods Med Res. 1999; 8: 135–60.

(30) Marquardt DW. An Algorithm for Least-Squares Estimation of Nonlinear Parameters. J Soc Indust

Appl Math. 1963; 11(2): 431-41.

(31)Riedmiller M, Braun H. A direct adaptive method for faster backpropagation learning: the RPROP algorithm. In: IEEE Int Conf Neural Netw; 1993; 1: 586-91.

(32)Hoerl AE, Kennard RW. Ridge regression: biased estimation for nonorthogonal problems. Technometrics. 1970; 12(1): 55-67.

Supplemental material

S1. Generalized Linear Model (GLM)

For standardized predictors $X \in \mathbb{R}^{N\times P}$ and target $y \in \mathbb{R}^{N}(\mathrm{Hb_{CPB}})$, we fit a Gaussian-identity GLM:

$$y = \beta_0 + X\beta + \varepsilon, \qquad \varepsilon \sim \mathcal{N}(0, \sigma^2 I). \tag{s-i}$$

Parameters (β_0, β) were estimated by maximum likelihood (equivalently, least squares under (i)).

Implementation used MATLAB fitglm (MathWorks) with default options.

S2. Support Vector Regression (SVR)

We used ε-SVR with radial basis function (RBF) kernel as shown in the following equation:

$$K(x_i, x_j) = \exp\left(-\frac{\| x_i - x_j\|^2}{2\sigma^2}\right). \tag{s-ii}$$

A ε-SVR model is obtained by solving the convex optimization problem as follows:

$$\min_{w,b,\xi,\xi^*} \frac{1}{2}\|w\|^2 + C\sum_{i=1}^{n} \xi_i + \xi_i^*, \tag{s-iii}$$

$$\text{subject to } \begin{cases} y_i - (w^T\phi(x_i) + b) \le \varepsilon + \xi_i, \\ (w^T\phi(x_i) + b) - y_i \le \varepsilon + \xi_i^*, \\ \xi_i, \xi_i^* \ge 0, \quad i = 1, \dots, n, \end{cases}$$

where ϕ is the mapping to the feature space, C is the penalty constant (BoxConstraint), and ε is the width of the epsilon-insensitive zone. The predicted Hb concentration $\hat{y}(x)$ is then expressed as a linear combination of support vectors, as follows:

$$\hat{y}(x) = \sum_{i\in \boldsymbol{S}} \alpha_i, K(x_i, x) + b\,, \qquad \boldsymbol{S} = \{i | \alpha_i \neq 0\}. \tag{s-iv}$$

We tuned $(C, \sigma, \gamma, \varepsilon)$ by cross-validation. Implementation used MATLAB fitrsvm with RBF kernel;

expected-improvement-plus criterion in 10-fold CV guided selection.

S3. Multilayer Perceptron (MLP)

We used a feed-forward network with $L-1$ hidden layers. For an input $x \in \mathbb{R}^P$, the layer outputs were defined as:

$$\mathbf{h}^{(l)} = \phi\left(\mathbf{W}^{(l)}\mathbf{h}^{(l-1)} + \mathbf{b}^{(l)}\right), \qquad \mathbf{h}^{(0)} = \mathbf{X}. \tag{s-v}$$

with the final prediction given by:

$$\hat{\boldsymbol{y}} = \mathbf{W}^{(L)}\mathbf{h}^{(L-1)} + \mathbf{b}^{(L)}, \tag{s-vi}$$

The weights $\{W^{(\ell)}, b^{(\ell)}\}$were learned by backpropagation using either the Levenberg–Marquardt or Resilient Backpropagation algorithm (31, 32), with learning rates 10^{-3}or $10^{-4}$and early-stopping patience of 10 or 20 epochs. Model selection followed a nested cross-validation scheme with 5 outer folds and a 5-fold inner grid search over hidden-layer sizes [4], [8], [16], [32], [32, 16], [64, 32], [128, 64], algorithm $\in$ {LM,RProp}, learning rate $\in \{10^{-3}, 10^{-4}\}$, and early-stopping tolerance $\in$ {10,20}. On the full standardized predictor matrix X, the selected configuration was [4] (one hidden layer with 4 neurons) trained with LM at a learning rate of 10^{-3}, early stopping of 10 epochs, and L2 weight decay of 0.1 (33); five random initializations were run and the model with the lowest validation MSE was retained.

S4. Dimensionality Reduction via PCA.

Continuous variables were z-score standardized and categorical variables were one-hot encoded. Principal component analysis (PCA) was then applied to the full predictor matrix to obtain the score matrix $P \in \mathbb{R}^{N \times P_{\mathrm{PCA}}}$. The retention rule was prespecified as "keep the smallest number of components whose cumulative explained variance reaches at least 90%." Component loadings were computed to support interpretability.

S5. Cross-validation, Metrics, and Comparative Baselines.

For model validation, SVR/MLP used standard train–validation splits with reporting on the final fit; SVR employed 10-fold cross-validation for hyperparameter selection and cross-validated error estimates; and MLP used nested 5×5 cross-validation for model selection with outer-fold performance reported. Model performance was summarized uniformly using R^2 and MSE, and agreement between predicted and measured values was assessed with Bland–Altman analysis (bias and 95% limits of agreement). Two published TBV-based formulas were included as comparative baselines; all models (baselines and proposed) were evaluated under the same preprocessing and validation procedures.